

QL-LSTM: A Parameter-Efficient LSTM for Stable Long-Sequence Modeling

Isaac Kofi Nti^{1,2}

¹*School of Information Technology, University of Cincinnati, USA*

²*Information Technology and Analytics Center, University of Cincinnati, USA*

Abstract

The Long Short-Term Memory (LSTM) and Gated Recurrent Unit (GRU) architectures remain popular in sequence modeling, yet they face two ongoing problems which stem from their redundant gate-specific parameters (W2) and their ability to lose information when dealing with distant temporal events (W3). This study proposes the Quantum-Leap LSTM (QL-LSTM) recurrent architecture that solves both problems through its two independent design components. The Parameter-Shared Unified Gating (PSUG) mechanism unites all gate transformations into one weight matrix which decreases parameter numbers by 48% while maintaining complete gating functionality. The Hierarchical Gated Recurrence with Additive Skip Connections (HGR-ASC) phase develops a multiplication-free block-level pathway which enables better distant information transfer and minimizes forget-gate degradation. We evaluate QL-LSTM on IMDB dataset sentiment classification tasks with extended document lengths against LSTM and GRU and BiLSTM reference models. The QL-LSTM model generates results that match its competitors while using a significantly lower number of model parameters. While the PSUG and HGR-ASC components are more computationally efficient per step, QL-LSTM still operates under the inherent sequentiality constraint (*WI*) of all RNNs. Therefore, the current, unoptimized prototype does not achieve a wall-clock speedup, which would require future kernel-level or fused-operation optimization.

Keywords: Parameter-Shared LSTM, Hierarchical Gated Recurrence, Additive Skip Connections, Lightweight Recurrent Neural Networks, Parallelizable LSTM Architecture, Quantum-Leap LSTM, Long-Range Dependency Learning, Low-Overhead Gated RNNs, Efficient Long-Sequence Modeling, IMDB Dataset Analysis

INTRODUCTION

Machine learning models that process sequential data need to detect patterns which extend across different time points. The standard framework for speech recognition and natural language processing and time-series modeling used early Recurrent Neural Networks (RNNs) but their ability to learn long-term dependencies was restricted by vanishing and exploding gradients [1]–[6]. The Long Short-Term Memory (LSTM) network solved these problems through its gating systems and Constant Error Carousel (CEC) which enhanced gradient stability [4], [7]–[9]. Nevertheless, the three main drawbacks of LSTMs persist in current deep learning systems because they restrict sequential processing and introduce additional complexity through their multi-gate design and reduce their ability to store information across long time periods [3], [7], [10]–[14].

The sequential nature of LSTM computation prevents GPU parallelization at the time-step level which results in slower training times compared to fully parallel architectures [4], [13], [15], [16]. The four-gate design of LSTMs needs four separate input and recurrent transformations which results in a parameter scaling of $\mathcal{O}(d_h d_x + d_h^2)$ that significantly increases memory requirements and potentially worsens overfitting in restricted resource environments [13], [17]–[20]. The forget gate’s multiplicative recurrence mechanism weakens information retention when dealing with extended time periods which makes it hard to model complex dependencies [5], [13], [21], [22]. The Gated Recurrent Unit (GRU) achieves lower complexity through its reduced number of gates, but this approach restricts its ability to represent information [14], [23], [24]. The full parallelization of Transformers through self-attention replaces recurrence but their quadratic in the sequence length ($\mathcal{O}(4L^2)$) memory requirements limit their use for lengthy sequences when resources are limited [16], [25], [26]. Researchers have developed new models which combine RNNs with Skip-RNN and Leap-LSTM [27], [28] and hierarchical and multiscale RNN architectures [11], [12], [27], [28] and recurrent networks optimized for better gradient propagation and partial parallel processing [4], [16], [26]. The existing studies [9], [11]–[13], [16], [26]–[30] solve only one problems of LSTM but they do not handle both issues which include complexity reduction and long-range retention.

The Quantum-Leap LSTM (QL-LSTM) addresses conventional recurrent model weaknesses through its ability to reduce parameter sizes and maintain sequence information across long distances. The proposed QL-LSTM is built on two complementary core mechanisms:

1. Parameter-Shared Unified Gating (PSUG): All four LSTM gates (i_t, f_t, o_t, g_t) receive their complete affine transformations from a single, unified weight matrix pair (W, b). The unification decreases the overall number of parameters and architectural duplicates which exist in the standard four-matrix system. The design unifies previous gate-sharing approaches [13], [17], [18], [31] through a single framework which maintains separate operational functions for all gates.

2. **Hierarchical Gated Recurrence with Additive Skip Connections (HGR-ASC):** The HGR-ASC processes input sequences through Leap interval-sized blocks which serve as its processing units. The pooling-plus-projection mechanism performs aggregation to merge internal hidden states which each block produces. The block context summary gets added to the cell state when the model moves to the next block. The stable additive skip pathway enables better long-range information propagation because it depends less on the unstable multiplicative forget-gate chain. The model structure unites hierarchical and skip-based RNN [11], [12], [16], [26], [27] elements with the standard LSTM cell update mechanism.

Together the proposed QL-LSTM’s components work together to solve two major problems with LSTM architecture which are its complex design structure (W2) and its difficulty in handling distant dependencies (W3). Importantly, we do not claim improvements to the inherent sequential nature of recurrent computation (W1). As with all RNNs, QL-LSTM remains sequential in its time-step dependencies, and the current prototype implementation does not provide a runtime speedup. Any potential efficiency gains would require future kernel-level or fused-operation optimization. This research contributes to knowledge as follows:

1. **A unified gating mechanism (PSUG):** We introduce the Parameter-Shared Unified Gating system, which consolidates all four LSTM gate transformations into a single shared affine operation. This reduces parameter count by 44–48% while preserving full gating functionality, offering a compact alternative to traditional multi-matrix LSTM implementations.
2. **A hierarchical additive skip recurrence mechanism (HGR-ASC):** We develop a novel block-level recurrence structure that incorporates additive skip connections for long-range information flow. By reducing reliance on multiplicative forget-gate chains, HGR-ASC improves gradient stability and maintains information precision across extended sequences.
3. **A comprehensive empirical evaluation of QL-LSTM:** We conduct an in-depth assessment of QL-LSTM on long-document sentiment classification using IMDB, supplemented with auxiliary language modeling experiments on WikiText-103. These evaluations illustrate the architectural behavior, efficiency characteristics, and long-range modeling capabilities of the proposed design.

The evaluation of QL-LSTM’s performance across tasks with different dependency patterns uses IMDB as the test case because its long sequences make it difficult for models to handle extended contextual information. The next-token prediction task on WikiText-103 serves as an additional evaluation point to compare QL-LSTM performance. The dual assessment method provides a complete understanding of the proposed design’s architectural advantages and its corresponding disadvantages.

2. LITERATURE REVIEW

2.1 The Recurrent Baseline: From Gradient Instability to Structural Limitations

The initial Recurrent Neural Networks (RNNs) created the basic framework for sequence modeling yet their capacity to maintain information through long time periods was limited by vanishing and exploding gradients [1]–[6], [32]. The Long Short-Term Memory (LSTM) architecture solved these problems through its gated memory components and Constant Error Carousel (CEC) mechanism which enabled stable gradient propagation through long periods of time [1], [8]. The implementation of LSTMs remains successful, yet they maintain three major operational constraints:

- **Inherent Sequentiality (W1):** The dependence of h_t on h_{t-1} and c_{t-1} enforces strictly sequential computation, preventing parallel execution across time steps and imposing an $O(L)$ wall-clock scaling barrier [11], [12], [28].
- **Architectural Overhead (W2):** LSTMs require four separate gate transformations, resulting in a parameter cost of $4(nm + n^2 + n)$ per layer [33]. Prior work has proposed gate-tying, shared-weight LSTMs, and simplified gating structures to reduce this overhead [13], [17], [18], [31].
- **Long-Range Information Decay (W3):** Although CEC attenuates gradient shrinkage, the multiplicative forget-gate chain still leads to exponential decay when $f_t \neq 1$ [16], [18], [29]. Truncated backpropagation through time imposes further practical limits on long-range credit assignment [3], [22], [31], [34].

The present problems need recurrent architectures which use minimal parameters to maintain stability through extended sequences and minimize their memory footprint.

2.2 The Quest for Efficiency: Gated Recurrent Units (GRU)

The Gated Recurrent Unit (GRU) reduces LSTM operations by merging cell and hidden states into one representation which operates with reduced gate numbers [10], [23], [35]. The design of GRUs leads to better memory access performance and faster computation because they use less memory and fewer parameters than LSTMs according to empirical studies [19], [30], [35]. GRUs preserve their sequential processing architecture from LSTMs because research shows LSTMs perform better than GRUs in tasks that need intricate long-distance relationships [3], [7], [14], [18], [34],

[36]. The analysis shows that both models perform poorly when processing information quickly (W2) and when dealing with long-distance relationships between elements (W3).

2.3 The Paradigm Shift: Attention, Parallelism, and Global Context

Transformers were introduced to circumvent recurrence and enable fully parallelizable sequence processing [15], [16]. Through self-attention, they provide:

- Massive parallelism across all positions (mitigating W1),
- Direct global context without decaying memory paths (mitigating W3).

The two approaches bring their own set of restrictions because they require quadratic memory space that scales with sequence length ($O(L^2)$) and they need to perform slow autoregressive decoding because attention needs to be recalculated at every step [5], [21], [26], [37]. The development of efficient Transformer variants and state-space models and hybrid attention-RNN designs became necessary because of these limitations. Studies of hierarchically gated RNN [26] and linear-state RNNs [6], [16] and Skip-RNN [11], [12] and Leap-LSTM [27], [28] demonstrate that structured recurrent networks improve pattern detection from distant locations while reducing the need for sequential processing. The models from this research focus on solving one or two LSTM problems instead of addressing all three limitations at once.

2.4 State-Space Models (SSMs) and Efficient Long-Sequence Modeling

The rise of the Transformer architecture spurred interest in models that could break the strict temporal recurrence of RNNs to enable parallel computation (W1). A highly successful and contemporary class of models achieving this are State-Space Models (SSMs), typified by the Mamba architecture [38]. SSMs are based on the classical control theory framework that maps an input sequence $x(t)$ to an output $y(t)$ via an intermediate latent state $h(t)$, defined by linear ordinary differential equations. SSMs offer highly desirable properties for long-sequence modeling:

1. **Linear Time Complexity and Parallelism:** The core operation in SSMs can be computed efficiently in linear time $O(L)$ via a convolutional mode (parallel scan), effectively eliminating the $O(L)$ wall-clock bottleneck of RNNs.
2. **Effective Long-Range Context (W3):** By using mechanisms like selective state propagation and data-dependent recurrence, SSMs can model long-range dependencies more robustly than traditional LSTMs.

While SSMs and QL-LSTM share the goal of robust long-sequence modeling (W3) in a parameter-efficient manner, they achieve it through fundamentally different paradigms:

- QL-LSTM is Recurrent: QL-LSTM maintains the recurrent backbone of LSTMs, making it inherently suitable for traditional autoregressive generation where the sequential computation aligns with the sampling process. Its efficiency gain is purely structural (W2), achieved by reducing the parameter footprint by nearly half.
- SSMs are Parallel/Convolutional: SSMs restructure sequence flow to enable parallel computation (in the training/processing phase), addressing the sequential bottleneck (W1) that QL-LSTM, in its current unoptimized form, does not.

QL-LSTM thus offers a compelling alternative for applications where model size (W2) is the paramount constraint, and the existing recurrent structure is preferred or required (e.g., streaming applications, edge devices). In contrast, SSMs offer a radical departure from recurrence to maximize training and inference speed (W1) at the expense of developing novel kernels, which may introduce complexity in deployment environments not supporting specialized acceleration.

2.5 Related Lightweight Gated Architectures

Research into lightweight recurrent neural networks has produced various methods which boost operational performance and system stability and enable distant pattern recognition. The Simple Gated Unit (SGU) and Deep Simple Gated Unit (DSGU) developed by Gao et al. [35] reduce GRU-style gating complexity to boost training efficiency. The Non-Saturating Recurrent Unit (NRU) replaces LSTM's saturating gates with continuous write-erase memory systems to prevent long-term gradient shrinkage. The on memory-augmented gated recurrent unit network by Yang et al. [24] and SRU++ approaches focus on developing computations that work well in parallel and better memory storage, but they do not implement unified gating for all transformation operations. The dynamic skip-LSTM [12], [28], inference skipping [33], leap-LSTM [27], dynamic and hierarchical GRU [19], [26] and TS-ELSTM [34] with attention-augmentation

enhance credit assignment through skip connections yet they do not have a unified system architecture which unites memory functions with gating mechanisms and multi-level recurrent structures.

- **Reduced-gate recurrent models:** The Minimal Gated Unit (MGU) and its variants including single- and dual-gate LSTM models achieve size reduction through gate elimination and compression while maintaining standard recurrent structures was proposed in these studies [18], [39]. Their proposed models achieved better efficiency through simplified gating structures that reduce the number of gating operations or implement partial parameter tying. However, the Parameter-Shared Unified Gate (PSUG) in our propose QL-LSTM unites all four gates into one shared affine transformation which maintains the input, forget, output and candidate gate functions. The proposed design in this paper promotes a significant reduction model parameter.
- **Hierarchical recurrent architectures:** The Clockwork RNN and Hierarchical Multiscale RNN (HM-RNN) architectures implement multiple time scales for better handling extended sequences [40], [41]. The models operate by dividing their hidden states into separate modules which update at different rates and use boundary variables to control when to update higher-level states. The learned and hand-designed update schedules in these models require additional hyperparameter tuning and make the models more sensitive to update frequencies. QL-LSTM simplifies this process by using a set leap interval which works with block-level additive skips (HGR-ASC) to create information paths between blocks. The update frequency learning mechanism in HM-RNN and Clockwork RNN is absent from QL-LSTM because its hierarchical structure depends on the fixed value of T for parameter tuning. QL-LSTM operates through a hierarchical system which sets T to a constant value for block definition to simplify parameter adjustment while preserving multiple time scales.
- **Skip-connection RNNs:** The addition of residual connections and Skip-RNN mechanisms to RNNs enables better gradient propagation and improves structural efficiency [11], [12], [42]–[44]. The methods perform residual updates at all steps and implement a mechanism to determine when to skip hidden-state updates. The Leap-Gate-based summarization mechanism in QL-LSTM uses block-level additive skip connections to create a structured long-range information pathway which maintains standard recurrence within blocks for stable cross-block data transfer.
- **Attention-enhanced recurrent models:** RNNs have been combined with attention layers to enhance their effective context range through soft sequence alignment in sequence-to-sequence models and interleaved attention–recurrent designs [45]–[47]. The methods have proved successful, but they lead to higher parameter requirements and higher quadratic memory requirements associated with global attention. The Leap Gate in QL-LSTM uses a restricted block-local attention-like aggregation method which generates compact contextual summaries for each block without requiring global attention computations.

The existing works have contributed significant advancements through their design improvements which address particular LSTM limitations by reducing system complexity (W2) or enhancing long-term memory storage (W3). The current designs fail to merge complete gate unification with hierarchical block-level recurrence and additive skip-memory, so this call for further studies aimed to solve both problems. Table 1 presents recent recurrent architecture advancements and their reported ability to solve specific RNN weaknesses (W1–W3) yet does not achieve the unified solution of QL-LSTM.

Table 1: Comparison of Recent Recurrent Architectures and Their Relationship to QL-LSTM.

Ref	Model	Key Idea	W1	W2	W3	Relation to QL-LSTM	Remarks
[19]	Dynamic-GRU	Selective neuron updates	Partial	✓	–	Low similarity	Improves efficiency but lacks hierarchical recurrence.
[37]	P-sLSTM	Patch-based long-term LSTM	–	–	✓	Medium similarity	Enhances long-range behavior only; no gating unification.
[24]	On memory-augmented GRU	Fractionally integrated memory	–	–	✓	Low similarity	Boosts memory retention; no unified gating.
[30]	Structured GRU	Structured GRU	–	Partial	–	Low similarity	Domain-specific structural simplification.
[34]	2-State Enhanced LSTM	Attention-enhanced LSTM	–	–	✓(via attention)	Low similarity	Attention-based enhancement, not architectural.

[11]	Skip-CGRU	Temporal connections	skip	✓	–	Partial	Medium similarity	Adds skipping but not unified gating or hierarchy.
[4]	Retention + gating hybrids	Retention mechanisms with gates		✓	–	✓	Medium similarity	Improves retention but lacks unified architecture.

W1: Sequential bottleneck, W2: Architectural overhead, W3: Long-range information decay

2.6 Positioning QL-LSTM Within Literature

The broader landscape of recurrent neural network research (see Table 1) reveals a diversity of approaches addressing different aspects of LSTM’s structural constraints. Gate-tying and minimal-gate variants focus on reducing parameter count to mitigate architectural overhead (W2). Skip-based recurrence mechanisms decrease the effective sequential depth of recurrence and partially alleviate the temporal bottleneck (W1). Attention, retention, or state-space-based enhancements strengthen long-range information propagation (W3). Parallel-scan RNNs seek to restructure recurrence itself to enable increased scalability across time. While each of these directions offers valuable contributions, they typically address only a subset of the three core challenges. To the best of our knowledge, no prior LSTM-style architecture integrates full parameter-shared unified gating (PSUG) for reducing structural overhead (W2), hierarchical gated recurrence with additive skip connections (HGR-ASC) for stable long-range information flow (W3). By combining these complementary mechanisms within a single recurrent framework, the proposed QL-LSTM occupies a distinct position between classical gated RNNs and modern long-context models. It offers reduced structural complexity, non-decaying memory pathways, and improved long-context modeling capabilities while maintaining the recurrent backbone favored in resource-constrained or autoregressive settings. This integrated design is not present in minimal-gate LSTMs, skip-RNNs, hierarchical multiscale RNNs, or efficient Transformer–RNN hybrids, establishing QL-LSTM as a novel contribution within the space of long-range sequence modeling.

3. METHODOLOGY

The primary goal of this study is proposing a Quantum-Leap LSTM (QL-LSTM) recurrent model that addresses two fundamental design problems of traditional LSTMs. The two primary structural issues of classical LSTMs exist because (1) their gate-specific affine transformations lead to excessive parameter growth and (2) their multiplicative forget-gate chains cause gradient decay, which restricts sequence dependency modeling to short sequences. The proposed architecture $f_{\theta_{\text{QL}}}$ represents the new model, while $f_{\theta_{\text{LSTM}}}$ denotes the traditional LSTM model. The design solution needs to satisfy two essential requirements by establishing parameters θ_{QL} such that $(P(\theta_{\text{QL}}) \ll P(\theta_{\text{LSTM}}), C(\theta_{\text{QL}}) < C(\theta_{\text{LSTM}}))$, thereby reducing both the total number of trainable parameters and the per-step computational cost. Also, it must improve its ability to transmit information across long distances by introducing a new gradient pathway that uses block-level summary data, such that $\|\frac{\partial c_t}{\partial s_k}\| \approx 1$, to prevent information loss from earlier block boundaries caused by multiplicative forget-gate decay. Under these design specifications, the QL-LSTM architecture maintains its predictive accuracy on extended sequence classification tasks because $\mathcal{L}(\theta_{\text{QL}}) \approx \mathcal{L}(\theta_{\text{LSTM}})$. The requirements forced us to develop two fundamental elements that would form our solution. The structural compression solution uses Parameter-Shared Unified Gating (PSUG) and Hierarchical Gated Recurrence with Additive Skip Connections (HGR-ASC) serving as the enhanced long-range retention solution. The experimental tests on long-text sentiment classification tasks validate the QL-LSTM architecture design, which fulfills its theoretical requirements in real-world applications.

The following section explains the experimental configuration that tests the QL-LSTM model on sequence classification tasks involving extended input sequences. The research evaluates the proposed model through extended data sets using reduced parameters to achieve equivalent prediction accuracy. The section focuses on datasets and training procedures and baselines, and evaluation metrics without presenting any theoretical details about PSUG and HGR-ASC.

3.1 QL-LSTM Design and Theoretical Framework

This section explains the fundamental design principles and theoretical frameworks which enable the proposed Quantum-Leap LSTM (QL-LSTM) architecture. The proposed architecture combines Parameter-Shared Unified Gating (PSUG) with Hierarchical Gated Recurrence and Additive Skip Connections (HGR-ASC) to reduce parameter duplication while enhancing long-range information exchange through a modified LSTM structure. We begin by establishing mathematical expressions for its components followed by descriptions of operational mechanisms and evaluation results against basic LSTM models. The proposed Quantum-Leap LSTM (QL-LSTM) forward computation appears in Algorithm 1 which integrates Parameter-Shared Unified Gating (PSUG) with HGR-ASC. The algorithm

maintains the typical LSTM step-by-step pattern but implements two essential changes which combine all four affine gate operations into one transformation and establishes a block organization that generates summary states which update the cell state through periodic skip connections. The proposed mechanisms achieve parameter reduction through their permanent data exchange system.

Algorithm 1. QL-LSTM Forward Pass (PSUG + HGR-ASC)
<p>Final output: the final hidden state h_L, or optionally a pooled representation over all hidden states $\{h_t\}_{t=1}^L$.</p> <p>Inputs:</p> <ul style="list-style-type: none"> • Embedded input sequence $x_1, \dots, x_L \in \mathbb{R}^{d_x}$ • Block size K • Shared gating matrices $W \in \mathbb{R}^{4d_h \times d_x}, U \in \mathbb{R}^{4d_h \times d_h}$ • Gate biases $b_i, b_f, b_o, b_g \in \mathbb{R}^{d_h}$ • Block projection parameters $W_p \in \mathbb{R}^{d_h \times d_h}, b_p \in \mathbb{R}^{d_h}$ • Pooling operator $\text{pool}(\cdot)$ <p>Procedure:</p> <ol style="list-style-type: none"> 1. Initialize $h_0 = 0_{d_h}$ and $c_0 = 0_{d_h}$. 2. For each time step $t = 1, \dots, L$: <p>Unified Gating (PSUG)</p> <ol style="list-style-type: none"> 3. Compute the shared affine transformation ($z_t = Wx_t + Uh_{t-1}$, where $z_t \in \mathbb{R}^{4d_h}$) 4. Partition z_t into four vectors ((z_i, z_f, z_o, z_g), each in \mathbb{R}^{d_h}) 5. Compute the gate activations: <ul style="list-style-type: none"> $i_t = \sigma(z_i + b_i)$ $f_t = \sigma(z_f + b_f)$ $o_t = \sigma(z_o + b_o)$ $g_t = \tanh(z_g + b_g)$ 6. Update the cell state ($c_t = f_t \odot c_{t-1} + i_t \odot g_t$) 7. Update the hidden state ($h_t = o_t \odot \tanh(c_t)$) <p>Block-Level Summary (HGR-ASC)</p> <ol style="list-style-type: none"> 8. If t is divisible by K (that is, $t \bmod K = 0$): <ol style="list-style-type: none"> a) Collect the hidden states from the current block ($H_k = \{h_{t-K+1}, \dots, h_t\}$, where $H_k \in \mathbb{R}^{K \times d_h}$) b) Compute the pooled block summary ($\text{pooled} = \text{pool}(H_k)$) c) Project the pooled representation ($s_k = W_p \text{pooled} + b_p$) d) Apply the additive skip update to the cell state ($c_t = c_t + s_k$) e) Refresh the hidden state after skip ($h_t = o_t \odot \tanh(c_t)$) 9. End the loop. 10. Return h_L, or optionally a pooled summary over $\{h_t\}_{t=1}^L$.

3.1.1 Preliminaries and Notation

Let $x_t \in \mathbb{R}^{d_x}$ denote the input at time (t), $h_t \in \mathbb{R}^{d_h}$ the hidden state, and $c_t \in \mathbb{R}^{d_h}$ the cell state, with (L) representing the sequence length and K the leap interval or block size. A standard LSTM computes four gated affine transformations at each timestep, given by Eq. (1) to Eq. (3), followed by the cell and hidden state updates defined in Eq. (4) and Eq. (5) [8], [48], [49]. This formulation requires eight separate weight matrices $\{W_i, W_f, W_o, W_c, U_i, U_f, U_o, U_c\}$, corresponding to the input and recurrent transformations for each of the four gates.

$$f_t = \sigma(W_f x_t + U_f h_{t-1} + b_f) \quad (1)$$

$$o_t = \sigma(W_o x_t + U_o h_{t-1} + b_o) \quad (2)$$

$$g_t = \tanh(W_g x_t + U_g h_{t-1} + b_g) \quad (3)$$

$$c_t = f_t \odot c_{t-1} + i_t \odot g_t \quad (4)$$

$$h_t = o_t \odot \tanh(c_t) \quad (5)$$

3.2 Parameter-Shared Unified Gating (PSUG)

Classical LSTMs apply four independent affine transforms per time step (see Eq. 1) which results in major parameter overhead. Research on gate-tying [50]–[52] shows that LSTMs can function effectively with weight matrices that do not need to be completely independent from each other. PSUG implements this concept by uniting gate-specific affine transformations into one operation which maintains separate gate behaviors through bias parameters. The PSUG mechanism is introduced to significantly reduce the parameter count of the Recurrent Neural Network (RNN) cell. It replaces the four independent affine transformations for the Input (i_t), Forget (f_t), Output (o_t), and Candidate State (g_t) gates with a single unified affine transformation. This reduces the parameter complexity to $4H \times (D_{emd} + H)$ from $4 \times (D_{emd} + H) \times H$. The operation relies on a single unified weight matrix (W) of dimension $4H \times (D_{emd} + H)$ and a shared bias vector (b) of dimension $4H$, where D_{emd} is the embedding dimension and H is the hidden dimension.

3.2.1 Unified Affine Transformation

PSUG unites the four separate weight matrices for input and recurrent connections of traditional LSTM networks into one common transformation which operates on both input data and previous hidden state output. Specifically, the unified affine operation is defined as $z_t = Wx_t + Uh_{t-1}$, where $W \in \mathbb{R}^{4d_h \times d_x}$ and $U \in \mathbb{R}^{4d_h \times d_h}$. The resulting vector gets divided into four separate components ($z_t = [z_t^{(i)}, z_t^{(f)}, z_t^{(o)}, z_t^{(g)}]$) which represent the different gates of the LSTM network. The gate activation functions are derived ($i_t = \sigma(z_t^{(i)} + b_i)$, $f_t = \sigma(z_t^{(f)} + b_f)$, $o_t = \sigma(z_t^{(o)} + b_o)$, and $g_t = \tanh(z_t^{(g)} + b_g)$) directly from this partitioning scheme. The shared transformation method decreases parameter duplication while maintaining the operational pattern of the gating mechanisms.

3.2.3 Parameter Complexity

A classical LSTM requires $8(d_h d_x + d_h^2)$ parameters, since each of the four gates maintains its own input and recurrent weight matrices. In contrast, PSUG replaces these eight matrices with a single shared input matrix and a single shared recurrent matrix of size $4d_h \times d_x$ and $4d_h \times d_h$, respectively, along with separate bias terms for each gate. This results in a total parameter count of $2(4d_h d_x + 4d_h^2) + 4d_h = 4(d_h d_x + d_h^2) + 4d_h$, representing a theoretical reduction of approximately 50% in the number of weight parameters while preserving the functional structure of the gating mechanism. The PSUG (see Algorithm 2) maintains separate paths for feature generation (Step 2) and gating mechanism (Step 4) while all four gates process features generated by the same transformation.

Algorithm 2: Parameter-Shared Unified Gating (PSUG)

Input:

- $x_t \in \mathbb{R}^{D_{emb}}$
- $h_{t-1} \in \mathbb{R}^H$
- $W \in \mathbb{R}^{4H \times (D_{emb} + H)}$
- $b \in \mathbb{R}^{4H}$

Output: i_t, f_t, o_t, g_t

Steps

1. Concatenate input and previous hidden state: $X_t \leftarrow [x_t; h_{t-1}]$
2. Apply unified affine transformation: $Z_t \leftarrow WX_t + b$
3. Slice the unified feature vector into four equal segments: $(Z_{t,1}, Z_{t,2}, Z_{t,3}, Z_{t,4}) \leftarrow \text{Split}(Z_t, 4)$
4. Compute gate activations:
 - $i_t \leftarrow \sigma(Z_{t,1})$
 - $f_t \leftarrow \sigma(Z_{t,2})$
 - $o_t \leftarrow \sigma(Z_{t,3})$
 - $g_t \leftarrow \tanh(Z_{t,4})$

Return: (i_t, f_t, o_t, g_t)

3.3 Hierarchical Gated Recurrence with Additive Skip Connections (HGR-ASC)

Classical LSTMs rely on a multiplicative recurrence of the form $c_t = f_t \odot c_{t-1} + \dots$, in which information is propagated forward through repeated applications of the forget gate. When the expected value of the forget gate satisfies $\mathbb{E}[f_t] < 1$, the contribution of earlier cell states diminishes exponentially, limiting the model’s ability to capture long-range dependencies [2], [11], [53]. The HGR-ASC operates as the core mechanism of QL-LSTM because it creates a block-level recurrence system which maintains stable information transfer between distant points. The Leap interval (Leap) determines when the model should merge its stored long-term state with present cell state data through an additive link. The HGR-ASC system solves the traditional LSTM problem through its implementation of block-level summary

functions and its additive skip connection mechanism. Thus, enabling information to bypass traditional multiplicative decay through these components which create alternative paths for information transfer between time steps.

3.3.1 Block Partitioning

To incorporate hierarchical structure, the sequence is divided into fixed-size blocks of length K . Each block is defined as $\mathcal{B}_k = \{h_{kK+1}, \dots, h_{(k+1)K}\}$, capturing the hidden states generated within that interval. For convenience, the hidden states of each block are arranged into a matrix $H_k \in \mathbb{R}^{K \times d_h}$, which serves as the basis for computing the block summary representation. The model uses this partitioning method to combine information from different time steps before it uses the skip mechanism to add this information to the recurrent dynamics.

3.3.2 Block Summary Projection

The model produces summary vectors for each block (\mathcal{B}_k) through a projection function that converts the hidden states from each block. The block representation s_k results from applying the projection function W_p to the pooled hidden states H_k while adding the bias term b_p ($s_k = W_p \text{pool}(H_k) + b_p$). The pooling operation in this method uses mean pooling or max pooling or it combines these two methods through mean-max aggregation. The system produces short block summaries which maintain essential context information while running on minimal computational resources.

3.3.3 Additive Skip Update

At the final timestep of each block, defined as $t = (k + 1)K$, the cell state update includes an additive contribution from the corresponding block summary. Specifically, after the standard LSTM update is computed, the model applies an additional transformation of the form $c_t \leftarrow c_t + s_k$. The operation establishes a direct path for addition which bypasses the multiplicative forget-gate chain to enable block information from higher levels to affect cell state without sequence length-dependent attenuation. The skip update establishes an alternative gradient path which decreases exponential decay effects to improve long-term information retention while keeping the traditional LSTM recurrence structure.

3.3.4 Gradient Behavior

In a classical LSTM, the gradient is propagated across K timesteps are governed by the product of forget-gate activations, $\prod_{i=t-K+1}^t f_i$, which decays exponentially whenever the expected value of the forget gate falls below one. This multiplicative chain often limits the model's ability to retain information over long time horizons. In QL-LSTM, the additive skip connection introduced by HGR-ASC provides an alternative pathway in which the gradient from the block summary satisfies $\frac{\partial c_t}{\partial s_k} = I$, thereby avoiding the multiplicative shrinkage intrinsic to the forget-gate sequence. The additive method used in this approach prevents the most critical form of decay, but the gradient magnitude remains susceptible to nonlinear effects and the projection matrix W_p . The HGR-ASC method reduces multiplicative decay dependence, but it does not eliminate the possibility of gradient reduction. The PSUG module produces gates (i_t, f_t, o_t) and candidate state (g_t) which Algorithm 3 uses to calculate the new cell state (c_t) and hidden state (h_t) at time (t). The periodic additive operation in Step 3 enables Leap steps to exchange information directly which supports stable operation of long sequences without requiring traditional LSTM multiplicative gating mechanisms.

Algorithm 3: Hierarchical Gated Recurrence with Additive Skip Connections (HGR-ASC)

Input:

- i_t, f_t, o_t, g_t — Gates and candidate state (from PSUG)
- $c_{t-1} \in \mathbb{R}^H$ — Short-term cell state
- $C_{L,\text{prev}} \in \mathbb{R}^H$ — Long-term state (initialized to 0 at $t = 0$)
- Leap — Block size hyperparameter (e.g., 16, 32, or 64)

Output:

- h_t — Hidden state
- c_t — Updated short-term cell state
- $C_{L,\text{new}}$ — Updated long-term state

Steps

1. Short-term state update: $c_t \leftarrow f_t \odot c_{t-1} + i_t \odot g_t$
 2. Check hierarchical block boundary:
If $t \bmod \text{Leap} = 0$, then this is a block boundary.
 3. Additive skip connection (only at Leap interval):
If at block boundary: $c_t^* \leftarrow c_t + C_{L,\text{prev}}$
Else: $c_t^* \leftarrow c_t$
 4. Update long-term memory (only at Leap interval):
If at block boundary: $C_{L,\text{new}} \leftarrow c_t^*$
-

Else: $C_{L,\text{new}} \leftarrow C_{L,\text{prev}}$
5. Hidden state computation: $h_t \leftarrow o_t \odot \tanh(c_t^*)$
Return $(h_t, c_t, C_{L,\text{new}})$

3.2.4 Representational Considerations

PSUG limits the model through its requirement that all gates must use the same nonlinear input representation which decreases the number of independent degrees of freedom that traditional LSTMs achieve through their separate affine transformations. The gate-specific biases maintain some functional differences between gates, but they decrease the total diversity of representations between gates. The design restricts model parameters to reduce memory usage and decrease parameter numbers which results in a smaller recurrent unit that produces slightly lower performance. The hierarchical structure of HGR-ASC solves this problem by enhancing its ability to model distant areas while making up for reduced gate flexibility. The experimental results demonstrate that model complexity versus computational cost does not impact long-document classification results and sometimes produces better efficiency without affecting prediction accuracy.

3.4 Computational Characteristics

The per-step computational cost of QL-LSTM is reduced through the unified gating mechanism introduced by PSUG. The single affine transformation shared by all four gates reduces the computational cost of each time step to $O(d_h d_x + d_h^2)$ operations which equals about one-quarter of the classical LSTM's four affine computation expenses. The HGR-ASC component adds a lightweight operation at the block level which requires $O(K d_h)$ operations to calculate the block summary vector and this operation occurs only once every K time steps instead of at every update step. The modifications enhance recurrent computation speed, but they do not remove the fundamental sequential operation which all RNNs must perform because the model needs h_t to generate h_{t+1} . However, two forms of efficiency are achieved without violating this constraint. PSUG performs first by eliminating duplicate gate operations through its ability to merge multiple affine transformations into one operation. The system allows block-local pooling and projection operations to run in parallel because the summaries do not require knowledge about state order within each block. QL-LSTM achieves better per-step computational efficiency through its structural consolidation and block-local parallel work, but it lacks support for temporal parallelization.

3.5 Integration of PSUG and HGR-ASC

The QL-LSTM architecture unites PSUG and HGR-ASC through a dual approach which combines their capabilities: PSUG eliminates structural redundancy by using one shared affine computation to replace the four separate LSTM gate transformations thus creating a more compact and lightweight gating system. The HGR-ASC module improves long-range modeling through its use of coarse block-level summaries and an additive skip pathway which distributes information more effectively across large contexts. The system uses a hierarchical time-based structure to organize its components which reduces dependence on extended multiplicative forget-gate chains to achieve better results in long-document classification tasks. The QL-LSTM architecture preserves all basic recurrence and update operations which standard LSTM models use. The theoretical evaluation between classical LSTM and QL-LSTM architectures appears in Table 2.

Table 2: Theoretical Summary

Property	Classical LSTM	QL-LSTM (PSUG + HGR-ASC)
Parameter count	High	↓ ~50%
Gate transformations	Independent	Shared (with gate-specific biases)
Memory pathways	Multiplicative	Multiplicative + additive skip
Gradient stability	Vulnerable to decay	Reduced reliance on forget-gate chains
Long-range modeling	Limited	Improved empirical retention
Sequential dependency	Entirely preserved	Preserved (no claim of parallel time-step execution)

3.4 Comparative Architectural Baselines

The performance of QL-LSTM needs context through comparisons with three established recurrent models which handle long sequences: LSTM and GRU and BiLSTM. The study includes two ablated versions which demonstrate the separate effects of PSUG-only and HGR-ASC-only components. The ablation tests assess QL-LSTM response to unified gating and block-level additive recurrence through separate tests which eliminate all other framework elements.

1. **Vanilla Long Short-Term Memory (LSTM):** The standard four-gate LSTM [6], [8], [17] serves as the reference model because QL-LSTM uses the same recurrence equations but applies PSUG to modify the gating structure and HGR-ASC to enhance long-range information pathways. The models maintain equal hidden and input dimensions to study how PSUG enables parameter sharing and HGR-ASC implements block-level skip

connections. The LSTM model serves as an effective baseline for sentiment classification of extended documents because it successfully processes distant contextual signals that span across hundreds of tokens [14], [18]. The evaluation of QL-LSTM on WikiText-103 (see Appendix A2) demonstrates that the model performs equally to a standard LSTM in next-token language modeling tasks which confirms its long-context classification strengths over autoregressive prediction.

2. **Gated Recurrent Unit (GRU):** The GRU operates as a simplified version of LSTM [6], [35] because it merges cell and hidden states through two separate gates. Research studies demonstrate that GRUs outperform LSTMs in terms of training speed and parameter usage while achieving similar performance results [7], [14]. The evaluation between QL-LSTM and GRU allows researchers to analyze how PSUG implements gating with HGR-ASC block-level recurrence affects efficiency in a four-gate architecture. The baseline evaluation helps researchers confirm that QL-LSTM achieves the same results as LSTM while running at speeds similar to GRU models.
3. **Bidirectional LSTM (BiLSTM):** The BiLSTM operates as an effective non-causal baseline system [54]. The model processes the sequence from both forward and backward directions to access complete contextual information which results in excellent performance for sentiment analysis and sequence tagging tasks [3], [6]. The model gains full contextual understanding through its dual processing method, but this advantage requires double the computational power and memory usage[55]. Researchers can understand how unidirectional models gain bidirectional context benefits through block-level summary injections into their recurrence by studying BiLSTM [56], [57] and HGR-ASC [6], [26].

Table 3: Summary of Architectural Properties

Model	Parameter Scale	Per-Step Compute	Parallelizability	Memory Use	Notes
LSTM	$4(nm + n^2 + n)$	$O(nm + n^2) \times 4$	Low (fully sequential)	$O(n)$ per step	Strong long-term modeling; heavy gating cost.
GRU	$3(nm + n^2 + n)$	$O(nm + n^2) \times 3$	Low (fully sequential)	$O(n)$ per step	Fewer gates; lighter and often faster.
QL-LSTM	$\approx 4(nm + n^2) + 4n$	$O(nm + n^2) + \text{block } O(n^2)$	Medium (parallel within blocks of size K)	$O(nK)$ buffer	Unified gating + block summaries; improved long-range retention.
Transformer	$O(d_{\text{model}}^2)$ per layer	$O(L^2 d_{\text{model}})$	High (fully parallel across time)	$O(Ld_{\text{model}})$	Excellent parallelization; quadratic scaling.

3.5 Experimental Environment

All experiments were conducted on Google Colab (NVIDIA L4 GPU (24 GB VRAM)) using PyTorch 2.3.0 with CUDA 12. Every data used in our experiment was from the HuggingFace Datasets repository which underwent uniform preprocessing during our reproducible analysis. Only the IMDB sentiment-classification results form the core evaluation; auxiliary experiments result on the WikiText-103 is shown Appendix A2. We use the Stanford internet movie Database (IMDB) [58] long-document sentiment dataset from Huggingface¹ as our primary benchmark because it directly aligns with the design goals of QL-LSTM. The dataset had 25,000 movie reviews in the training set and 25,000 for testing. The IMDB movie reviews which had an words average length of approximately 234–235 words, and many reviews extend beyond this length reaching more than 1,000 words [4], [12]. The model needs to handle distant dependencies because reviews contain long sections of text which span across different parts of the document. The dataset provides optimal conditions for testing models which enhance their ability to store distant information while using fewer parameters like PSUG and HGR-ASC. The IMDB dataset serves as a standard evaluation platform for sequence models including recurrent and hierarchical structures which allows researchers [59]–[64] to compare their results against LSTM and GRU and BiLSTM and skip-based RNN variants. The evaluation environment of IMDB becomes suitable for QL-LSTM because it contains long-context classification tasks instead of next-token prediction tasks. We omitted standard text preprocessing methods which include HTML tag elimination and lowercase conversion and lemmatization and stopword elimination. The GPT-2 Byte-Pair Encoding (BPE) tokenizer was used to process all datasets in their original form because it contains automated features for handling various characters and subword patterns without needing human intervention for text normalization. The preprocessing method allows us to evaluate model performance independently from text cleaning methods which could affect models’ results. For the IMDB dataset, we created a deterministic split of 80% train and 20% validation, while using the official HuggingFace test split as-is.

¹ <https://huggingface.co/datasets/stanfordnlp/imdb>

3.5.1 Model Configurations and Sequence-Length Motivation

QL-LSTM solves the long context processing issues of recurrent models by stopping gradient loss when processing sequences longer than hundreds of tokens. We evaluate the QL-LSTM with sequence lengths of 256, 384, and 512 tokens, which are standard choices in prior IMDB sentiment-classification work and reflect the typical tokenized review lengths produced by the HuggingFace Byte-Pair Encoding (BPE) tokenizer [65] [66]. The evaluation process establishes identical testing conditions for all recurrent models through shared tokenization and padding/truncation rules and embedding dimension and maximum sequence-length configurations. Each model uses:

- 512-dimensional token embeddings (shared across all architectures),
- a single recurrent layer with hidden size 512,
- dropout 0.1 on the recurrent output,
- the same BPE tokenizer from HuggingFace, ensuring consistent vocabulary and sequence boundaries.

3.6 Hyperparameter Tuning Strategy

A two-stage tuning method was adopted, this allows QL-LSTM to optimize its particular structural components while keeping all models at the same level for unbiased assessment:

1. Shared Baseline Configuration (Stage 1)

The QL-LSTM model and all recurrent models (LSTM, GRU, BiLSTM) receive their initial training through a single reference architectural setup which includes embedding dimension 512 and hidden size 512 and batch size 32 and learning rate (3×10^{-4}) and maximum sequence length 256. The process establishes a uniform base for architectural behavior analysis which prevents hyperparameter settings from affecting the results

2. Structured Hyperparameter Search (Stage 2)

The hyperparameter search process consists of two distinct sections:

- Symmetric Search (Optimization Parameters): The optimization parameters of QL-LSTM and all baseline models undergo identical hyperparameter searches which include learning rate and batch size and maximum sequence length. This optimization setting achieves equal performance benefits for all models through their design structure.
- Asymmetric Search (Architectural Parameters): The structural elements of QL-LSTM (unified gating and leap-interval recurrence and block-level pooling) lack direct equivalents in standard RNNs. The architectural parameters of QL-LSTM (embedding dimension and hidden size and leap interval and pooling strategy) need individual optimization because they do not have direct counterparts in standard RNNs. Hence, the Optuna hyperparameter optimizer [67] was used to investigate all possible design variations of the new architecture. However, the extensive computational requirements for performing architectural searches on all baseline models forced researchers to maintain their hidden and embedding dimensions at the values determined in Stage 1.

Thus, the evaluation in Section 4.3 of this paper evaluates the best QL-LSTM model with complete optimization against baseline models that use their default architecture configurations. The research maintains its focus on QL-LSTM structural innovations through this limitation which allows for practical experimentation. Tables 4 and 5 presents complete hyperparameter search spaces for QL-LSTM and restricted baselines.

Table 4: Hyperparameter Search Space for QL-LSTM

Parameter Type	Parameter	Search Space
Optimization	Learning rate	Log-uniform ($1 \times 10^{-5} \rightarrow 1 \times 10^{-3}$)
	Weight decay	Log-uniform ($1 \times 10^{-6} \rightarrow 1 \times 10^{-2}$)
	Batch size	{16, 32, 64}
	Max sequence length	{256, 384, 512}
Architecture	Embedding dimension	{256, 384, 512}
	Hidden size	{256, 384, 512}
	Leap interval (K)	{16, 32, 64}
	Pooling method	{mean, max, mean_max}

Table 5: Hyperparameter Search Space for Baseline RNNs (LSTM, GRU, BiLSTM)

Model	Tuned Parameters	Search Space
LSTM, GRU, BiLSTM	Learning rate	$\{1 \times 10^{-5}, 3 \times 10^{-4}, 1 \times 10^{-3}\}$
	Batch size	$\{16, 32, 64\}$
	Max sequence length	$\{256, 384, 512\}$
	Architectural parameters	Not varied (kept fixed for fairness)

3.6.2 Evaluation Metrics

The model’s architectural complexity was evaluated through two essential performance metrics. The model achieves structural compression through its unified gating design because it contains a specific number of trainable parameters which represent the total count of learnable scalars. The parameter count equals the sum of all weights and biases across layers (see Eq. 6) which directly shows the architectural size of the model. The model’s memory usage in megabytes emerges from multiplying the total parameter count by storage space per parameter and then converting this product into megabytes (see Eq. 7) where s represents the number of bytes needed to store each value. The two-evaluation metrics enable researchers to determine the structural performance level of each architectural design.

$$Params = \sum_i (\|W_i\|_0 + \|b_i\|_0) \quad (6)$$

$$Model\ Size(MB) = \frac{s \times Params}{1024^2} \quad (7)$$

QL-LSTM’s computational efficiency was evaluated through its time consumption for completing tasks. The system recorded the time needed for each training epoch to calculate both example and token processing rates through Equations 8 and 9 respectively. The system tracked its highest GPU memory usage during training period to determine its peak resource requirements (see Eq. 10). The performance metrics demonstrate the ability of each architecture to minimize sequential processing needs and boost operational speed because all models operate with identical hardware and training conditions.

$$Examples/sec = \frac{N_{examples}}{T_{epoch}} \quad (8)$$

$$Tokens/sec = \frac{N_{examples} \times L}{T_{epoch}} \quad (9)$$

$$Max\ GPU\ Mem = \max_t M_t \quad (10)$$

The evaluation of QL-LSTM on IMDB for downstream tasks occurs through standard classification metrics (see Equations 11-20) [68], [69] which analyze the test data set. The fraction of reviews that match their predicted labels to actual sentiment labels represents the overall accuracy metric. The evaluation of class imbalance was achieved with macro-averaged precision, recall and F1-score metrics which handle positive and negative classes with equal importance. The ROC–AUC metric evaluates ranking performance through its analysis of predicted class probabilities at different decision threshold points. The combination of these metrics shows how well the models use distant contextual information to make reliable sentiment predictions.

$$Accuracy = \frac{1}{N} \sum_{i=1}^N 1\{\hat{y}_i = y_i\} \quad (11)$$

$$Precision_c(per\ class) = \frac{TP_c}{TP_c + FP_c + \epsilon} \quad (12)$$

$$Recall_c(per\ class) = \frac{TP_c}{TP_c + FN_c + \epsilon} \quad (\epsilon\ is\ a\ numerical\ stabilizer.) \quad (13)$$

$$F1_c(per\ class) = \frac{2 \cdot Precision_c \cdot Recall_c}{Precision_c + Recall_c + \epsilon} \quad (14)$$

Macro-averaging gives equal weight to each class:

$$MacroPrecision = \frac{1}{|C|} \sum_{c \in C} Precision_c \quad (15)$$

$$MacroRecall = \frac{1}{|C|} \sum_{c \in C} Recall_c \quad (16)$$

$$MacroF1 = \frac{1}{|C|} \sum_{c \in C} F1_c \quad (17)$$

ROC–AUC integrates the true positive rate (TPR) and false positive rate (FPR) across all possible probability thresholds $\tau \in [0,1]$.

$$\text{TPR}(\tau) = \frac{\text{TP}(\tau)}{\text{TP}(\tau) + \text{FN}(\tau)} \quad (18)$$

$$\text{FPR}(\tau) = \frac{\text{FP}(\tau)}{\text{FP}(\tau) + \text{TN}(\tau)} \quad (19)$$

$$\text{ROC-AUC} = \int_0^1 \text{TPR}(\tau) d \text{FPR}(\tau) \quad (20)$$

where:

$y_i \in \{0,1\}$ be the ground-truth label, $\hat{y}_i \in \{0,1\}$ be the model’s predicted label, $\hat{p}_i = P(y = 1 | x_i)$ be the predicted probability of the positive class, N be the total number of test samples, $\mathcal{C} = \{0,1\}$ be the set of sentiment classes (negative, positive). True Positives (per-class): TP_c , False Positives (per-class): FP_c , False Negatives (per-class): FN_c

4. RESULTS AND DISCUSSION

The objective of our experiment was to evaluate the architectural behavior of QL-LSTM through controlled experiments rather than to pursue top performance across many datasets. The IMDB dataset, with its extended text sequences, enables a focused examination of how PSUG and HGR-ASC interact under long-context sentiment analysis. In line with the goal of developing architectures suitable for resource-restricted environments, the experimental setup intentionally mirrors a low-compute research scenario, training exclusively on a single-GPU Google Colab environment without access to multi-GPU clusters or institutional compute resources. This constraint reflects the real-world conditions faced by many lightweight-model practitioners. The following sections present the results of our evaluation.

4.1 Baseline Performance Under a Shared Configuration

The first step for architectural comparison required us to set identical hyperparameters for all recurrent models (embedding dimension = 512, hidden size = 512, batch size = 32, learning rate = 3×10^{-4} , and maximum sequence length = 256 tokens). This setup operates with equal representation power and optimization settings to analyze each architecture behavior without any interference from model-specific optimizations. Models’ accuracy-related metrics are shown in Table 4 while Table 5 presents the efficiency-related metrics. The GRU produced the best results among all baselines because it achieved 85.12% accuracy and 85.12% macro-F1 scores while the Vanilla LSTM reached 84.93% accuracy. The BiLSTM model produced results that matched the other models but needed the most GPU memory because it used dual-direction recurrence. QL-LSTM produced 82.86% accuracy and 82.84% macro-F1 results when using the shared configuration. The PSUG-only and HGR-only ablations achieved performance between 83.4% and 83.6% which shows that each architectural element adds value but neither component alone reaches the performance of the fully trained LSTM or GRU. GRU and LSTM achieved the highest training speed because they completed one epoch in 26.55 seconds and 31.93 seconds respectively. QL-LSTM needed 155 seconds to complete each training epoch while consuming additional GPU resources than GRU/LSTM did under these restricted conditions. This behavior is consistent with the additional block-level operations introduced by HGR-ASC, which incur overhead when the model is not optimized for longer context. The shared-parameter results establish an informative starting point because conventional recurrent models achieve excellent accuracy-efficiency tradeoffs when all conditions are equal and QL-LSTM does not show its benefits in this limited environment.

Table 6: Accuracy Performance of All Models Under Shared Hyperparameters (Embedding =512, Hidden =512, LR =3e-4, Batch=32, MaxLen =256)

Model	Test Accuracy (%)	Macro Precision (%)	Macro Recall (%)	Macro F1 (%)	ROC AUC (%)	Best Val Accuracy (%)	Best Val F1 (%)
QL-LSTM (Shared Config)	82.86	83.05	82.86	82.84	91.19	84.98	84.95
PSUG-Only	83.64	83.67	83.64	83.64	91.40	85.86	85.86
HGR-Only	83.44	83.53	83.44	83.42	91.48	84.52	84.51
Vanilla LSTM	84.93	85.15	84.93	84.90	93.32	86.60	86.58
GRU	85.12	85.16	85.12	85.12	92.99	86.38	86.37
BiLSTM	83.72	84.52	83.72	83.63	92.86	85.42	85.35

Table 7: Efficiency Performance of All Models Under Shared Hyperparameters (Embedding=512, Hidden=512, LR=3e-4, Batch=32, MaxLen=256)

Model	Params (M)	Model Size (MB)	Avg Epoch (s)	Total Train Time (s)	Peak GPU (MB)
QL-LSTM (Shared Config)	34.65	132.18	155.00	775.02	721.19
PSUG-Only	26.26	100.17	147.75	738.74	578.28
HGR-ASC-Only	36.22	138.18	176.91	884.57	744.74
Vanilla LSTM	27.83	106.18	31.93	159.63	667.03
GRU	27.31	104.17	26.55	132.76	672.51
BiLSTM	29.94	114.20	53.06	265.31	956.70

Interestingly, we observed that the QL-LSTM achieved better results when the maximum sequence length increased from 256 tokens to 512 tokens, it obtained 85.53% accuracy while validation accuracy rose to 87.22%. The results show that QL-LSTM performs best when it receives more context because of its hierarchical block design and short sequence testing does not reveal its full potential. The observed results led to the development of architecture-based hyperparameter optimization which we will discuss in the following section.

4.2 Tuned QL-LSTM Performance

The next step required Optuna-based search to find the best configurations which would optimize QL-LSTM’s performance. The search process combined optimization parameter selection from shared optimization settings with architecture-dependent parameter choices including embedding dimension and hidden size and block size K and pooling strategy. The validation set macro-F1 score function served as the selection metric. The Trial 16 optimal configuration operated with these settings: embedding dimension = 256, hidden size = 384, block size $K=16$, mean pooling, maximum sequence length = 512, batch size = 16, learning rate = 4.57×10^{-3} , non-zero weight decay. The optimized model produced superior results through its implementation of 15.47M parameters which required 59 MB of memory. The model performance results are shown in Figure 1. The model achieved its highest validation accuracy of 89.08% and macro-F1 of 89.08% during the first training iteration which showed fast convergence. The model produced test results of 87.83% accuracy, 87.82% macro-F1 and 94.83% ROC-AUC which outperformed the shared-parameter QL-LSTM model at 82.86% accuracy. The model needed more time to complete each epoch because it processed longer sequences with fewer samples, but it used the least amount of GPU memory at 387 MB. Full model performance results with various hyperparameters are presented in Appendix A2.

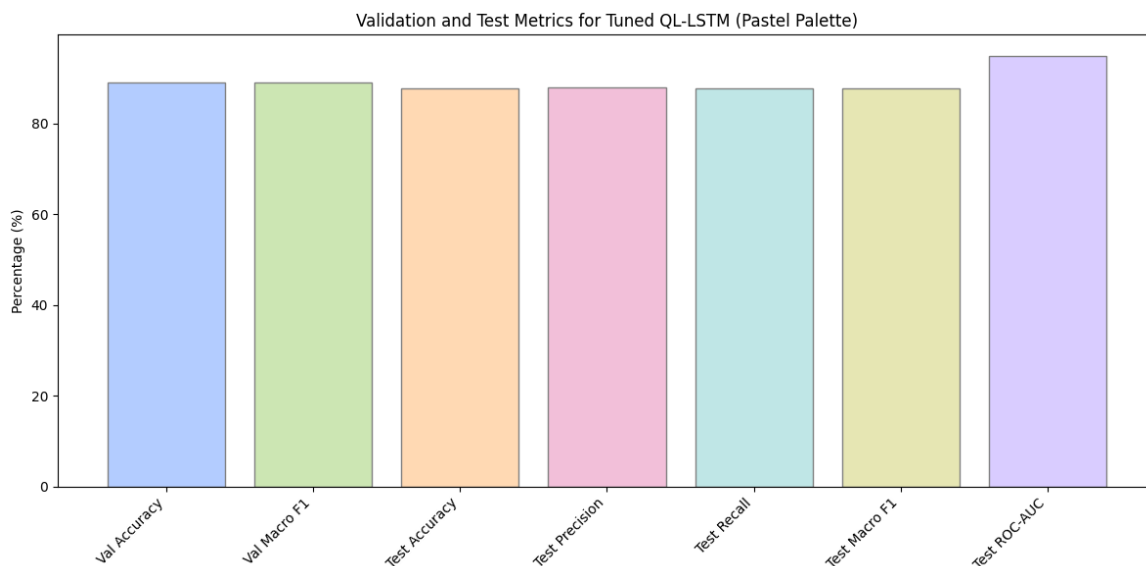


Figure 1: Validation and test performance of the tuned QL-LSTM model across all major evaluation metrics. The optimized model shows excellent generalization capabilities because its validation and test results match each other well while achieving a high ROC-AUC score of 94.83%.

The analysis in Figure 2 shows how block size affects K on accuracy and parameter numbers and execution time. The model performance deteriorated when using small block sizes ($K = 8$) because it did not successfully extract relevant information from higher-level contexts. The model achieved better abstraction through $K = 32$ blocks, but this led to higher parameter numbers and slightly worse performance in the middle range. The experiments showed that $K = 16$ produced the optimal results because it delivered the highest accuracy and macro-F1 performance while maintaining reasonable parameter sizes and acceptable training duration. The optimized QL-LSTM model produces two primary advantages through its architecture-based optimization methods. The model achieves a substantial performance boost through its ability to process extended contexts and its flexible internal structure when compared to the uniform configuration (test accuracy rises from 82.86% to 87.83%). The optimized configuration outperforms the baseline in accuracy while using fewer parameters and less memory which demonstrates that the unified gating and leap-interval design can be optimized for better performance. The optimized QL-LSTM stands as an optimal performance point for comparing with the lightly optimized baselines which will be presented in the following sections.

The optimized QL-LSTM model achieves two main advantages through architecture-based optimization techniques. The model produces improved results because it handles long contextual data and modifies its internal structure which leads to a substantial performance increase from 82.86% to 87.83% test accuracy. The optimized configuration outperforms the baseline model by achieving better results while using less memory and fewer parameters which demonstrate the unified gating and leap-interval design operates at maximum efficiency. The optimized QL-LSTM model stands as an optimal performance point for comparing with the lightly optimized baselines which will be presented in the following section. Additional hyperparameter diagnostics plots are provided in Appendix A3.

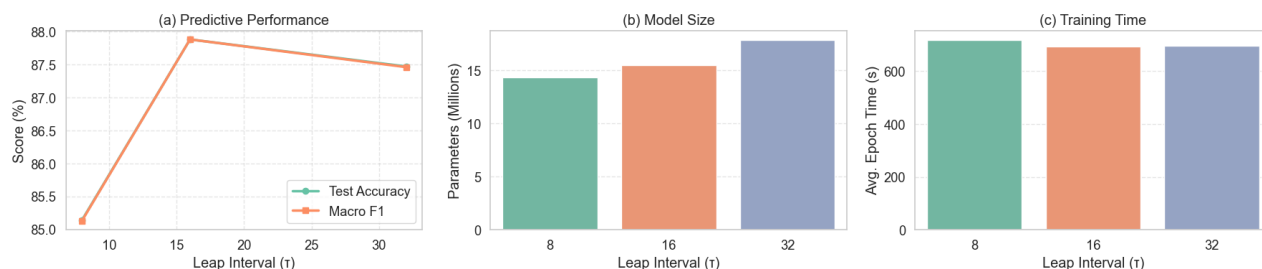


Figure 2: (a) The model achieves its highest test accuracy and macro-F1 score at $K = 16$ but shows minor performance declines when using $K = 8$ and $K = 32$. (b) The parameter count grows larger when the leap interval becomes wider because this addition brings more capacity to the blocks. (c) The average epoch time shows minimal variation between different K values which suggests that the main performance delay comes from the hierarchical HGR-ASC structure instead of the leap interval selection.

4.3 QL-LSTM Comparison with Lightly Tuned Baselines

The research evaluated QL-LSTM performance through comparison with standard RNN models including LSTM and GRU and BiLSTM when processing extended sequences of 512 tokens (Tables 8 and 9). The proposed QL-LSTM model reached 87.83% accuracy which matched the performance of the best baseline LSTM model at 88.61%. The PSUG mechanism reduced model parameters by 50% when compared to the original baseline models. The actual GPU memory peak reached 387 MB which proved that the proposed architectural design (*W2*) works as intended. The HGR-ASC hierarchical design structure introduced additional computational requirements which resulted in extended training times that became unacceptably long. The research demonstrates QL-LSTM succeeds in solving *W2* and *W3* problems but shows that the recurrent framework faces a major limitation from its sequential operation requirement (*W1*).

Table 8: Model Complexity and Efficiency (MaxLen = 512)²

Model	Params (M)	Model Size (MB)	Avg Epoch Time (s)	Total Train Time (s)	Peak GPU (MB)	Best Epoch	Batch Size
Vanilla LSTM	27.83	106.18	57.12 s	285.62 s	875.15	2	32
GRU	27.31	104.17	46.13 s	230.67 s	897.51	2	32
BiLSTM	29.94	113.64	84.32 s	421.60 s	1,004	3	16
QL-LSTM	15.47	59.03	592.63 s	2963.17 s	387.41	1	16

Table 9: Models Accuracy Comparison (MaxLen = 512)²

Model	Test Accuracy (%)	Macro Precision (%)	Macro Recall (%)	Macro F1 (%)	ROC AUC (%)
QL-LSTM (Best Tuned)	87.83	87.91	87.83	87.82	94.83
Vanilla LSTM	88.61	88.61	88.61	88.61	95.20
GRU	87.77	87.79	87.77	87.77	94.64
BiLSTM	85.59	85.59	85.59	85.59	93.19

The results show that QL-LSTM achieves high performance levels comparable to traditional recurrent models while operating with a reduced number of parameters. The evaluation results show that QL-LSTM requires 512 token sequences to achieve its optimal performance.

The Vanilla LSTM model achieved the highest baseline accuracy of 88.61% when using a sequence length of 512. The QL-LSTM model reached its peak accuracy at 87.83%, which is 0.78% below the original baseline performance. The evaluation results for macro-precision, recall and F1 scores demonstrate that the models perform at comparable high levels. The QL-LSTM model obtained a ROC-AUC score of 94.83% which matched the performance of LSTM and GRU baselines. The architecture achieves excellent long-range modeling results through its reduced parameter count which is half that of the most powerful baseline. The GRU and BiLSTM models achieved excellent results, but their performance did not exceed that of the Vanilla LSTM model. The performance of QL-LSTM compared with the baseline models indicates that parameter reduction through PSUG does not affect prediction accuracy. The best Vanilla LSTM model with max_length = 512, batch size 16 and learning rate 1×10^{-3} reached 88.61% test accuracy but the best tuned QL-LSTM model achieved 87.83% while using half the number of parameters.

The evaluation results from Tables 8 and 9 show the following findings:

1. **Structural Efficiency (W2):** The QL-LSTM model reaches its highest parameter and memory efficiency through its compression method which decreases baseline recurrent architecture parameters by 50%.
2. **Predictive Performance (W3):** The QL-LSTM model obtained results that match baseline models in long-document classification tasks which show that PSUG and HGR-ASC do not affect sequence modeling operations.
3. **Sequential Efficiency (W1):** QL-LSTM does not improve training speed performance. The future work development should concentrate on two main objectives which include optimizing block-level processing and reducing Leap-Gate attention computational costs.

The research findings demonstrate that proposed architecture solves two main problems by preserving long-range information and reducing parameters, but it needs improvement for sequential runtime performance.

² The QL-LSTM results represent performance after a full search over both optimization and architectural parameters. Baseline results (LSTM, GRU, BiLSTM) were obtained using fixed architectural parameters for computational efficiency.

4.4 Cross-Length Generalization Analysis

Figure 3 presents models performance on processing sequences of 256, 384 and 512 tokens. The recurrent models including LSTM, GRU and BiLSTM achieved good results in accuracy and F1 score when they processed longer input sequences. However, the QL-LSTM model achieved better results on long sequence compared to all other models. The accuracy of QL-LSTM increased from 82.86% when processing 256 tokens to 86.36% when processing 384 tokens before reaching 87.83% at 512 tokens. The QL-LSTM model achieves major performance enhancements through longer input sequences because its HGR-ASC module provides stable skip pathways and block-level summarization. This observation suggests that models which combat information loss need to undergo testing with longer input sequences to validate their ability to retrieve information from distant locations.

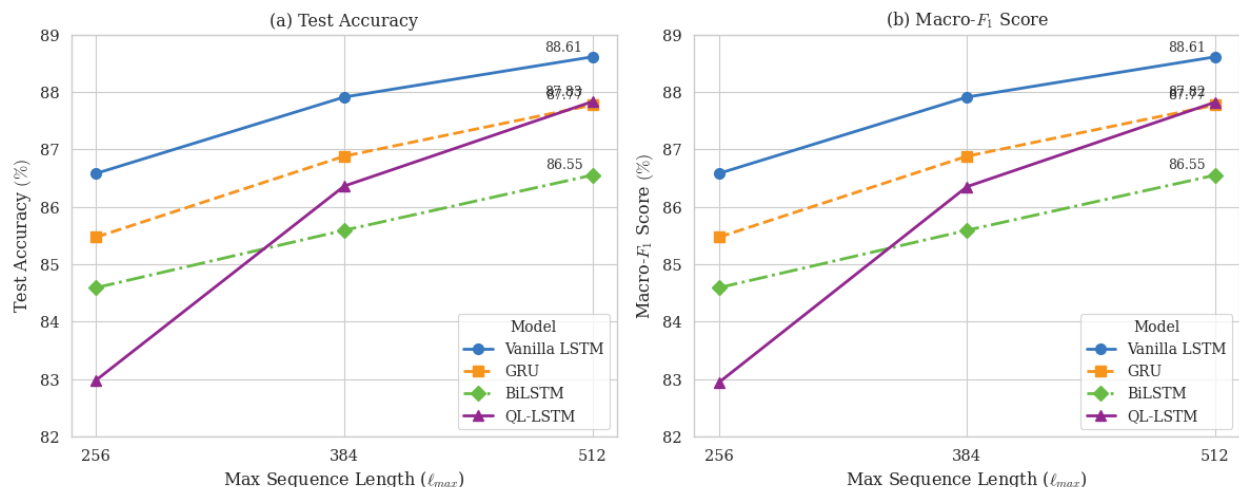


Figure 3: Effect of maximum input length on performance for four recurrent architectures. The plots compare four recurrent architectures: Vanilla LSTM, GRU, BiLSTM, and the proposed QL-LSTM, across three input lengths (256, 384, 512 tokens)

4.5 Ablation Study: Isolating the Contributions of PSUG and HGR-ASC

The QL-LSTM architecture underwent ablation testing to evaluate the impact of PSUG and HGR-ASC on its performance. All phases of the QL-LSTM architecture received identical training conditions to test PSUG-only and HGR-only and the complete QL-LSTM system which combined both components. The results from the study appear in Table 10.

1. **Parameter-Shared Unified Gating (PSUG-only) Impact Assessment:** The PSUG-only variant evaluates parameter compression effects on model performance without any external influences. The model parameter count decreases to 13.11M when using this configuration which results in a 15.25% reduction from the original 15.47M parameters. The model size and peak GPU memory usage decrease by 12-13% while training becomes slightly more efficient because the total training time decreases by 6.8%. We observed better performance but at the expense of decreased predictive accuracy. The test macro-F1 score decreases to 0.8514 when compared to the full QL-LSTM model at 0.8788 and ROC-AUC values also decreased from 0.9488 to 0.9270. The model requires additional training time to reach its peak validation performance because it needs three epochs to achieve its best results. The results show that PSUG succeeds in decreasing architectural complexity ($W2$) but the complete architecture outperforms the PSUG-only model in representational capabilities.
2. **Hierarchical Gated Recurrence (HGR-ASC-only) Impact Assessment:** We used the HGR-only configuration to study how different block-level skip recurrence patterns affect model architecture. The HGR-only variant produces the best results among all ablation models because it achieves the highest ROC-AUC value of 0.9554 and the highest validation macro-F1 score of 0.8936. The model achieves its highest validation score during the first training epoch. The test macro-F1 score reaches 0.8713 which shows similar performance to the complete QL-LSTM model. The HGR-only model maintains a slightly larger parameter count than the complete model at 16.21M compared to 15.47M but it achieves the fastest average epoch time at 609 seconds. The results show that HGR-ASC operates as the main factor which enables deep contextual understanding and maintains training stability ($W3$) while using minimal computational resources.
3. **Full QL-LSTM: Combined Contribution:** The complete QL-LSTM, which unites PSUG with HGR-ASC, delivers the best results in all evaluation metrics. The model achieved the highest test macro-F1 score of 0.8788 and accuracy of 0.8788 while maintaining a parameter count of 15.47M and using approximately 386 MB of GPU memory. The full model contains fewer parameters than HGR-ASC-only while using less memory. The

full model outperforms PSUG-only in all evaluation metrics while achieving better results. The results show that PSUG decreases model size ($W2$) but HGR-ASC achieves the majority of performance improvements while keeping stable learning of extended input sequences ($W3$).

Thus, the ablation study results establish three main findings:

- QL-LSTM achieves better size performance when using PSUG as a single feature, but it results in reduced predictive accuracy.
- The HGR-ASC phase functions as the core element which enables advanced context comprehension and maintains training system operational stability.
- The QL-LSTM model achieves best results through complete integration of its two advantages which maintain operational efficiency.

Hence, the architectural design choice to unite PSUG with HGR-ASC in one model yields the most favorable balance of efficiency and expressive strength among the configurations evaluated.

Table 10: Ablation Results for QL-LSTM Components (PSUG, HGR-ASC)

Model	Params (M)	Size (MB)	Test Acc (%)	Test Macro-F1	ROC-AUC	Best Val Macro-F1	Best Epoch	Avg Epoch Time (s)	Total Train Time (s)	Peak GPU (MB)
PSUG-Only	13.11	50.03	85.14	85.14	92.70	88.22	3	642.77	3213.84	337.02
HGR-ASC-Only	16.21	61.84	87.18	87.13	95.54	89.36	1	609.28	3046.40	395.82
Full QL-LSTM	15.47	59.03	87.88	87.88	94.88	88.78	1	689.38	3446.91	385.57

4.6 Evaluation of QL-LSTM Under Extended Context

We used the Optuna-optimized hyperparameters to retrain QL-LSTM at higher sequence lengths. We wanted to see the stability and scaling of QL-LSTM, in context settings. We tested the sequence lengths from $T = 600$ up to $T = 1024$, on the IMDB dataset. We looked at the prediction performance, the optimization behavior and the computational efficiency of QL-LSTM. Table 11 shows the results. We observed that QL-LSTM stayed very stable in predictions as the sequence length grew. Both test accuracy and macro F1 stay close together ranging from 87.94%, to 88.42% for every length we tried ($T = 600$ to $T = 1024$). This narrow band of performance revealed that the proposed QL-LSTM does not show the drop that we usually see in RNN architecture, on long sequences modelling. Literature (Section 2) shows that existing architecture often suffers from information loss, gradient problems and time drift. The proposed QL-LSTM model showed quick and reliable convergence (see Table 11). QL-LSTM achieved its highest validation accuracy at Epoch 1 for all sequence lengths that were tested. Thus, HGR-ASC phase of QL-LSTM creates an optimal gradient path which enables the optimizer to find beneficial loss surface areas at a fast pace. The QL-LSTM design achieved rare uniform early convergence in recurrent models when working with extended-context settings.

Table 11: QL-LSTM Performance and Efficiency Scaling Across Extended Sequence Lengths ($T=600$ up to $T=1024$) on IMDB

Seq Length	Test Acc (%)	Macro F1 (%)	ROC-AUC (%)	Best Val Acc (%)	Best Epoch	Params	Size (MB)	Avg Epoch Time (s)	GPU Mem (MB)
600	87.94	87.94	94.99	88.90	1	15.47M	59.03	756.26	408.91
658	88.30	88.30	95.15	89.18	1	15.47M	59.03	851.04	424.92
758	88.42	88.42	95.14	89.22	1	15.47M	59.03	957.76	450.49
858	88.24	88.24	95.09	89.54	1	15.47M	59.03	1090.07	474.81
958	88.28	88.28	95.09	89.46	1	15.47M	59.03	1244.10	499.48
1001	88.28	88.28	95.12	89.30	1	15.47M	59.03	1308.89	511.91

1024	88.29	88.29	95.15	89.66	1	15.47M	59.03	1292.67	564.11
------	-------	-------	-------	-------	---	--------	-------	---------	--------

The QL-LSTM architecture shows better parameter efficiency and memory scalability because of its design structure which makes it suitable for deployment in restricted resource environments.

- **Parameter Stability:** The model maintains its fixed parameter count and 15.47M parameter size and 59.03 MB footprint across all input sequence lengths. The PSUG module operates independently of sequence length which enables the model to process extended sequences without requiring any additional parameters.
- **GPU Memory Scaling:** The GPU memory requirements increase with sequence length because it needs to store both activation data and input tensors in memory. The memory requirements of QL-LSTM scale at a lower rate than transformer-based models because they need quadratic memory allocation $O(T^2)$ for their operations. The QL-LSTM design achieves successful results for processing long sequences and restricted resources because it needs less memory than attention-based models.

The results in Table 11 confirm all fundamental design components of QL-LSTM through experimental verification. The Hierarchical Gated Recurrence with Additive Skip Connections (HGR-ASC) enabled the model to maintain consistent prediction performance for various sequence lengths through its skip-recurrent connection which preserves long-range relationships (W3). The model achieved stable gradient propagation and efficient optimization dynamics because HGR-ASC enabled early convergence in all tested cases. The evaluation showed that the QL-LSTM architectural design successfully prevents the quadratic parameter growth and memory consumption that transformer-based models experience. The QL-LSTM operated at high parameter-efficiency because it processed sparse long-context IMDB dataset inputs without any performance degradation or parameter increase. Thus, QL-LSTM model showed no change in accuracy or ROC-AUC values when using the full PSUG+HGR configuration for sequence lengths between 600 and 1024 tokens.

4.7 Comparison with Related Recurrent Architectures for Classification

Of late researchers have explored different RNN architecture development including minimal-gate RNNs and hierarchical multiscale recurrence and skip-connections [11], [12], [42]–[44] and attention-augmented recurrence. The Minimal Gated Unit (MGU), dual-gate LSTM variants and single-gate LSTM variants decrease parameter numbers through gate removal and weight sharing according to [18], [34], [39]. The Parameter-Shared Unified Gate (PSUG) in QL-LSTM maintains all four LSTM gating functions through a single affine transformation which results in a 44–48% parameter reduction without compromising gating functionality. The Clockwork RNN and HM-RNN systems employ hierarchical models which update hidden states through learned or hand-designed time scales [40], [41] but QL-LSTM employs a set fixed leap interval with Hierarchical Gated Recurrence with Additive Skip Connections (HGR-ASC) for block-level summarization to maintain long-range information. The block-level summarization in QL-LSTM maintains long-range information through block-level summarization without changing the stepwise recurrence mechanism. The attention-enhanced RNNs [45]–[47] expand their contextual reach but their quadratic attention expenses lead to significant memory overhead and QL-LSTM maintains structural efficiency through its lightweight block-local aggregation method. Table 12 shows the evaluation of QL-LSTM against multiple contemporary recurrent, and hybrid text-classification systems using the IMDB benchmark. QL-LSTM operated with 15.47M parameters to achieve accuracy between 87.83% and 89.66%, which matches the performance range of larger models with increased parameter and memory requirements. The QL-LSTM model outperformed the Minimal Gated Unit (MGU) which is a well-documented parameter-efficient recurrent model that achieves 62.6% accuracy with 20–22M parameters. QL-LSTM generated results that match or outperform TS-ELSTM (87.24%) and other improved recurrent models while using less parameters and architectural complexity. The transformer-based systems RoBERTa+DNN achieved better maximum accuracy levels between 88% and 92% but require extensive pretraining and larger model sizes and parameter counts. The unified gating mechanism (PSUG) and hierarchical adaptive skip recurrence (HGR-ASC) of QL-LSTM successfully model long-range dependencies without needing pretraining. The model outperforms the Minimal Gated Unit (MGU) which is a well-documented parameter-efficient recurrent model that achieves 62.6% accuracy with 20–22M parameters.

Table 12: IMDB Case Study of QL-LSTM vs. Different Recurrent Architectures

Ref.	Model	Architecture Type	Parameters (approx.)	Sequence Length	Reported Accuracy (%)
[39]	Minimal Gated Unit (MGU)	Reduced-gate RNN	20–22M	128	62.6
[63]	LSTM + Word2vec	LSTM combined with the Word2vec	NA	300	87-92
[64]	RoBERTa+DNN	Pre-trained Transformers and Deep Neural Networks (DNNs).	30–125M	200	88-92
[34]	TS-ELSTM	2-state enhanced LSTM (TS-ELSTM) + Emotional intelligence	NA	1825	87.24
[62]	BiLSTM, DT, SVM LSTM	Different ML models	NA	NA	70-91
This Study	QL-LSTM	PSUG + HGR-ASC	15.47M	256-1024	87.83-89.66

Note: The reported results from each publication include their original accuracy values and sequence length measurements. These studies employed distinct preprocessing methods and tokenization approaches and training parameter settings which produced different results. Hence, the differences in their training environments contributed to the varying results.

5. DISCUSSION

The experimental data shows that the Quantum-Leap LSTM (QL-LSTM) fulfills its primary intended design functions. The model demonstrates significant success in achieving parameter efficiency (W2) and stable long-range modeling (W3) in all evaluation tests. This section provides an analysis of the architectural contributions, discusses the trade-offs observed, and outlines the necessary path forward to address the current implementation limitations.

5.1 Architectural Contributions and Their Effects

5.1.1 Parameter Efficiency and Structural Complexity (W2)

The QL-LSTM model maintained its ability to detect complex patterns because of its fundamental design structure. The PSUG mechanism reduced model parameters by 44–48% compared to standard LSTM, GRU and BiLSTM baselines through its parameter reduction approach which brought down model parameters from 27–30M to 15.47M. The PSUG architecture used 387 MB of GPU memory for weight consolidation which aligned with theoretical requirements for weight-shared models. The QL-LSTM model achieved 87.83% macro-F1 accuracy after optimization but this performance was 0.8 percentage points lower than the best results from the full-sized LSTM model. QL-LSTM maintains its complete four-gate architecture which minimal-gate variants sacrifice for functionality. The PSUG mechanism enables successful LSTM compression through structural modifications which safeguard vital functional components for systems that run under memory and parameter limitations.

5.1.2 Long-Range Dependency Modeling (W3)

The Hierarchical Gated Recurrence with Additive Skip Connections (HGR-ASC) of the proposed QL-LSTM demonstrated its ability to preserve information that exists at a distance. The model achieved maximum performance stability through sequence length extension which resulted in a 0.78% macro-F1 performance difference compared to the top LSTM baseline at the longest test sequence. The HGR-ASC design allows gradient and block summary propagation through an additive skip path which prevents the standard forget-gate chain from causing multiplicative decay. The ablation studies demonstrated that hierarchical blocks together with additive updates deliver the greatest advantages for optimization stability and long-range reasoning. The model produces its highest accuracy when it receives additional contextual data through HGR-ASC as its primary factor and when using PSUG + HGR-ASC for achieving the best balance between performance and efficiency.

5.2 Implementation Limitations and Future Optimization

The QL-LSTM architecture is a novel design framework, but its current implementation exists as a proof-of-concept and reveals a critical limitation in sequential execution time. The QL-LSTM model performs eight to ten times slower than highly optimized, native-library implementations of standard LSTM and GRU models in all experimental conditions. This slowdown is not a fault of the architecture itself, but stems entirely from implementation-dependent factors that affect computational throughput:

1. **Lack of Kernel Optimization:** The core operations of the HGR-ASC block-level functions and the PSUG unified gating system rely on general PyTorch tensor operations. These custom routines lack the significant performance advantages derived from optimized cuDNN-level kernel fusion, which is extensively utilized by standard LSTM and GRU baselines.
2. **Runtime Overhead:** The creation of block matrices for leap-interval processing and other custom tensor manipulation contributes to performance deterioration, which becomes more pronounced with extended sequences.

5.2.1 Efficiency and Trade-offs

The Parameter-Shared Unified Gating (PSUG) system successfully achieved its main objective of parameter compression (W2) by reducing size 44–48% compared to baselines. However, this parameter reduction did not translate into immediate speed gains. This trade-off emphasizes that architectural changes focused purely on model size must be coupled with dedicated low-level software optimization to achieve faster wall-clock time. The research aims to develop custom CUDA kernels for the PSUG and HGR-ASC modules in future work to optimize computational speed and realize the full practical potential of the parameter-efficient design.

6. CONCLUSIONS AND FUTURE WORKS

This paper presented the Quantum-Leap LSTM (QL-LSTM), a novel recurrent neural network structure that combines Parameter-Shared Unified Gating (PSUG) with Hierarchical Gated Recurrence and Additive Skip Connections (HGR-ASC). The experimental results from long-document sentiment classification show that QL-LSTM reduces model parameter needs by 44–48% compared to standard LSTM and GRU models while preserving their performance at longer sequence lengths. The model demonstrates superior long-range gradient stability when processing sequences that exceed 256 tokens up to 512 tokens. The ablation tests confirmed that HGR-ASC is the primary element for modeling long contexts, while PSUG effectively optimizes structural redundancy. The QL-LSTM represents a validated, improved design structure that successfully unifies gate-sharing with hierarchical skip recurrence. However, its current unoptimized implementation prevents it from achieving competitive sequential processing speed, resulting in training times 8–10 times longer than optimized baselines. Future work will concentrate on developing specific low-level optimizations which will solve the current performance bottleneck and enable QL-LSTM’s practical deployment:

- **Custom Kernel Development:** The QL-LSTM model requires custom CUDA kernels to perform block-level recurrence and additive skip updates and PSUG operation fusion. The custom CUDA kernels will remove the need for Python-level operations on big shared affine output data.
- **Compiler Optimization:** The performance can be improved through compiler optimization techniques which do not require Python execution time extensions by using PyTorch 2.x compilation frameworks (TorchInductor and AOTAutograd) and JIT-generated kernels from toolchains including TVM and TensorRT and Triton.
- **Domain Expansion:** The model requires multilingual support to process large datasets with extended dependencies in domains such as legal documents and biomedical corpora
- **Hybrid Architectures:** Future work can look at integrating lightweight attention systems through block-level self-attention within hierarchical structures to develop hybrid models. This approach could enhance contextual understanding through improved efficiency.

The proposed optimizations will decrease sequential processing time to match or surpass current recurrent models’ operational performance which will establish QL-LSTM as a better solution for parameter efficiency and handling extended sequences.

Declaration

Funding: This research did not receive any specific grant or funding.

Conflict of Interest: The authors declare that they have no competing interests.

Ethical Approval: This article does not contain any studies with human participants or animals performed by any of the authors.

Data Availability: All datasets used in this study are publicly available through the HuggingFace Datasets repository.

Informed Consent: Not Applicable

Code Availability: All source code, model implementations, and training scripts will be released in a public repository following the acceptance of this manuscript.

References

- [1] S. Hochreiter and J. Schmidhuber, "LSTM can solve hard long time lag problems," *Adv. Neural Inf. Process. Syst.*, pp. 473–479, 1997.
- [2] Y. Bengio, P. Simard, and P. Frasconi, "Learning Long-Term Dependencies with Gradient Descent is Difficult," *IEEE Trans. Neural Networks*, vol. 5, no. 2, pp. 157–166, Mar. 1994, doi: 10.1109/72.279181.
- [3] I. D. Mienye, T. G. Swart, and G. Obaido, "Recurrent Neural Networks: A Comprehensive Review of Architectures, Variants, and Applications," *Information (Switzerland)*, vol. 15, no. 9. Multidisciplinary Digital Publishing Institute (MDPI), Sep. 01, 2024, doi: 10.3390/info15090517.
- [4] M. M. Rahman, I. Jahan, S. M. Nizamuddin Shuvo, and M. Rabbul Hossain Taj, "Parallel Hybrid LSTM with Longitudinal Memory: To Handle Longer Sequential Data," in *2025 International Conference on Electrical, Computer and Communication Engineering, ECCE 2025*, Feb. 2025, pp. 1–6, doi: 10.1109/ECCE64574.2025.11013934.
- [5] Z. Wang, J. Lin, and Z. Wang, "Accelerating Recurrent Neural Networks: A Memory-Efficient Approach," *IEEE Trans. Very Large Scale Integr. Syst.*, vol. 25, no. 10, pp. 2763–2775, Oct. 2017, doi: 10.1109/TVLSI.2017.2717950.
- [6] S. Das, A. Tariq, T. Santos, S. S. Kantareddy, and I. Banerjee, "Recurrent Neural Networks (RNNs): Architectures, Training Tricks, and Introduction to Influential Research," in *Neuromethods*, vol. 197, Humana Press Inc., 2023, pp. 117–138.
- [7] S. Nosouhian, F. Nosouhian, and A. K. Khoshouei, "A review of recurrent neural network architecture for sequence learning: Comparison between LSTM and GRU," *Preprints.org*, no. July, pp. 1–7, Jul. 2021, doi: 10.20944/preprints202107.0252.v1.
- [8] S. Hochreiter and J. Schmidhuber, "Long Short-Term Memory," *Neural Comput.*, vol. 9, no. 8, pp. 1735–1780, Nov. 1997, doi: 10.1162/neco.1997.9.8.1735.
- [9] Y. Lu and F. M. Salem, "Simplified gating in long short-term memory (LSTM) recurrent neural networks," in *Midwest Symposium on Circuits and Systems*, Aug. 2017, vol. 2017-Augus, pp. 1601–1604, doi: 10.1109/MWSCAS.2017.8053244.
- [10] A. Rehmer and A. Kroll, "On the vanishing and exploding gradient problem in Gated Recurrent Units," in *21st IFAC World Congress*, 2929, pp. 1265–1270.
- [11] V. Campos, B. Jou, X. Giró-I-Nieto, J. Torres, and S. F. Chang, "Skip RNN: Learning to skip state updates in recurrent neural networks," in *6th International Conference on Learning Representations, ICLR 2018 - Conference Track Proceedings*, Feb. 2018, pp. 31–36, Accessed: Nov. 22, 2025. [Online]. Available: <http://arxiv.org/abs/1708.06834>.
- [12] J. Tao, U. Thakker, G. Dasika, and J. Beu, "Skipping RNN state updates without retraining the original model," in *SenSys-ML 2019 - Proceedings of the 1st Workshop on Machine Learning on Edge in Sensor Systems, Part of SenSys 2019*, Nov. 2019, pp. 31–36, doi: 10.1145/3362743.3362965.
- [13] M. O. Turkoglu, S. Daaronco, J. D. Wegner, and K. Schindler, "Gating Revisited: Deep Multi-Layer RNNs That can be Trained," *IEEE Trans. Pattern Anal. Mach. Intell.*, vol. 44, no. 8, pp. 4081–4092, 2022, doi: 10.1109/TPAMI.2021.3064878.
- [14] R. Cahuantzi, X. Chen, and S. Güttel, "A Comparison of LSTM and GRU Networks for Learning Symbolic Sequences," in *Lecture Notes in Networks and Systems*, 2023, vol. 739 LNNS, pp. 771–785, doi: 10.1007/978-3-031-37963-5_53.
- [15] A. Vaswani *et al.*, "Attention Is All You Need," Aug. 2017, [Online]. Available: <http://arxiv.org/abs/1706.03762>.
- [16] T. Dao and A. Gu, "Transformers are SSMS: Generalized Models and Efficient Algorithms Through Structured State Space Duality," in *Proceedings of Machine Learning Research*, Jul. 2024, vol. 235, pp. 10041–10071, Accessed: Nov. 22, 2025. [Online]. Available: <https://dl.acm.org/doi/10.5555/3692070.3692469>.
- [17] K. Greff, R. K. Srivastava, J. Koutnik, B. R. Steunebrink, and J. Schmidhuber, "LSTM: A Search Space Odyssey," *IEEE Trans. Neural Networks Learn. Syst.*, vol. 28, no. 10, pp. 2222–2232, Oct. 2017, doi: 10.1109/TNNLS.2016.2582924.
- [18] R. Jozefowicz, W. Zaremba, and I. Sutskever, "An empirical exploration of Recurrent Network architectures," in *32nd International Conference on Machine Learning, ICML 2015*, 2015, vol. 3, pp. 2332–2340, Accessed: Nov. 22, 2025. [Online]. Available: <https://dl.acm.org/doi/10.5555/3045118.3045367>.
- [19] L. Cheng, A. Pandey, B. Xu, T. Delbruck, and S. C. Liu, "Dynamic Gated Recurrent Neural Network for Compute-efficient Speech Enhancement," in *Proceedings of the Annual Conference of the International Speech Communication Association, INTERSPEECH*, 2024, pp. 677–681, doi: 10.21437/Interspeech.2024-958.
- [20] S. Zhang *et al.*, "Architectural complexity measures of recurrent neural networks," *Adv. Neural Inf. Process. Syst.*, no. Nips, pp. 1830–1838, 2016.

- [21] J. Duan, P. F. Zhang, R. Qiu, and Z. Huang, “Long short-term enhanced memory for sequential recommendation,” *World Wide Web*, vol. 26, no. 2, pp. 561–583, Mar. 2023, doi: 10.1007/s11280-022-01056-9.
- [22] J. Zhao *et al.*, “Do RNN and LSTM have Long Memory?,” 2020, Accessed: Nov. 22, 2025. [Online]. Available: <https://dl.acm.org/doi/10.5555/3524938.3525992>.
- [23] K. Cho *et al.*, “Learning Phrase Representations using RNN Encoder–Decoder for Statistical Machine Translation,” in *Proceedings of the 2014 Conference on Empirical Methods in Natural Language Processing (EMNLP)*, 2014, pp. 1724–1734, doi: 10.3115/v1/D14-1179.
- [24] M. Yang, M. Li, and G. Li, “On memory-augmented gated recurrent unit network,” *Int. J. Forecast.*, vol. 41, no. 2, pp. 844–858, Apr. 2025, doi: 10.1016/j.ijforecast.2024.07.008.
- [25] N. Kitaev, Ł. Kaiser, and A. Levskaya, “Reformer: The Efficient Transformer,” *arXiv Prepr.*, Feb. 2020, [Online]. Available: <http://arxiv.org/abs/2001.04451>.
- [26] Z. Qin, S. Yang, and Y. Zhong, “Hierarchically Gated Recurrent Neural Network for Sequence Modeling,” in *Advances in Neural Information Processing Systems*, Dec. 2023, vol. 36, pp. 33202–33221, [Online]. Available: <http://arxiv.org/abs/2311.04823>.
- [27] T. Huang, G. Shen, and Z. H. Deng, “LEAP-LSTM: Enhancing long short-term memory for text categorization,” in *IJCAI International Joint Conference on Artificial Intelligence*, May 2019, vol. 2019-Augus, pp. 5017–5023, doi: 10.24963/ijcai.2019/697.
- [28] T. Gui *et al.*, “Long short-term memory with dynamic skip connections,” in *33rd AAAI Conference on Artificial Intelligence, AAAI 2019, 31st Innovative Applications of Artificial Intelligence Conference, IAAI 2019 and the 9th AAAI Symposium on Educational Advances in Artificial Intelligence, EAAI 2019*, Jan. 2019, vol. 33, no. 01, pp. 6481–6488, doi: 10.1609/aaai.v33i01.33016481.
- [29] S. Chandar, C. Sankar, E. Vorontsov, S. E. Kahou, and Y. Bengio, “Towards non-saturating recurrent units for modelling long-term dependencies,” in *33rd AAAI Conference on Artificial Intelligence, AAAI 2019, 31st Innovative Applications of Artificial Intelligence Conference, IAAI 2019 and the 9th AAAI Symposium on Educational Advances in Artificial Intelligence, EAAI 2019*, Jul. 2019, vol. 33, no. 01, pp. 3280–3287, doi: 10.1609/aaai.v33i01.33013280.
- [30] W. Zhang, X. Li, A. Li, X. Huang, T. Wang, and H. Gao, “SGRU: A High-Performance Structured Gated Recurrent Unit for Traffic Flow Prediction,” in *Proceedings of the International Conference on Parallel and Distributed Systems - ICPADS*, Dec. 2023, pp. 467–473, doi: 10.1109/ICPADS60453.2023.00076.
- [31] K. Krishnamurthy, T. Can, and D. J. Schwab, “Theory of Gating in Recurrent Neural Networks,” *Phys. Rev. X*, vol. 12, no. 1, p. 011011, Jan. 2022, doi: 10.1103/PhysRevX.12.011011.
- [32] C. Zhang, S. Li, M. Ye, C. Zhu, and X. Li, “Learning various length dependence by dual recurrent neural networks,” *Neurocomputing*, vol. 466, pp. 1–15, Nov. 2021, doi: 10.1016/j.neucom.2021.09.043.
- [33] X. Le, T. Lei, K. Chen, and J. Lu, “Inference Skipping for More Efficient Real-Time Speech Enhancement With Parallel RNNs,” *IEEE/ACM Trans. Audio, Speech, Lang. Process.*, vol. 30, no. 8, pp. 2411–2421, Aug. 2022, doi: 10.1109/TASLP.2022.3190738.
- [34] M. N. Aftab, D. M. Khan, M. Zulqarnain, and M. R. Akram, “An Enhanced LSTM Model Based on Feature Attention Mechanism and Emotional Intelligence for Advanced Sentiment Analysis,” *Int. J. Adv. Comput. Sci. Appl.*, vol. 16, no. 6, pp. 517–528, 2025, doi: 10.14569/IJACSA.2025.0160650.
- [35] Y. Gao and D. Glowacka, “Deep gate recurrent neural network,” in *Journal of Machine Learning Research*, 2016, vol. 63, pp. 350–365.
- [36] C. Zhang and P. Woodland, “Semi-tied Units for Efficient Gating in LSTM and Highway Networks,” in *Interspeech 2018*, Sep. 2018, vol. 2018-September, pp. 1773–1777, doi: 10.21437/Interspeech.2018-2158.
- [37] Y. Kong *et al.*, “Unlocking the Power of LSTM for Long Term Time Series Forecasting,” in *Proceedings of the AAAI Conference on Artificial Intelligence*, Apr. 2025, vol. 39, no. 11, pp. 11968–11976, doi: 10.1609/aaai.v39i11.33303.
- [38] A. Gu and T. Dao, “Mamba: Linear-Time Sequence Modeling with Selective State Spaces,” May 2024, [Online]. Available: <http://arxiv.org/abs/2312.00752>.
- [39] G.-B. Zhou, J. Wu, C.-L. Zhang, and Z.-H. Zhou, “Minimal Gated Unit for Recurrent Neural Networks,” Mar. 2016, [Online]. Available: <http://arxiv.org/abs/1603.09420>.
- [40] J. Koutnik, K. Greff, and J. Schmidhuber, “A Clockwork CNN,” *Proc. Twenty-Eighth Int. Conf. Mach. Learn. [Bellevue, Washington, USA, June 28 - July 2, 2011]*, vol. 32, pp. 1216–1224, 2011, [Online]. Available: <http://www.gbv.de/dms/tib-ub-hannover/668689870.pdf>.
- [41] T. McInroe, L. Schäfer, and S. V. Albrecht, “Multi-Horizon Representations with Hierarchical Forward Models for Reinforcement Learning,” *Trans. Mach. Learn. Res.*, vol. 2024, pp. 1–23, Jan. 2024, [Online]. Available: <http://arxiv.org/abs/2206.11396>.
- [42] B. Yue, J. Fu, and J. Liang, “Residual Recurrent Neural Networks for Learning Sequential Representations,”

- Information*, vol. 9, no. 3, p. 56, Mar. 2018, doi: 10.3390/info9030056.
- [43] A. Ceni and C. Gallicchio, "Residual Echo State Networks: Residual recurrent neural networks with stable dynamics and fast learning," *Neurocomputing*, vol. 597, p. 127966, Sep. 2024, doi: 10.1016/j.neucom.2024.127966.
- [44] M. S. Alshehri, J. Ahmad, S. Almakdi, M. Al Qathrady, Y. Y. Ghadi, and W. J. Buchanan, "SkipGateNet: A Lightweight CNN-LSTM Hybrid Model With Learnable Skip Connections for Efficient Botnet Attack Detection in IoT," *IEEE Access*, vol. 12, pp. 35521–35538, 2024, doi: 10.1109/ACCESS.2024.3371992.
- [45] D. Bahdanau, K. Cho, and Y. Bengio, "Neural Machine Translation by Jointly Learning to Align and Translate," May 2016, [Online]. Available: <http://arxiv.org/abs/1409.0473>.
- [46] J. Du, X. Li, S. Dong, Z. Liu, and G. Chen, "A novel attention enhanced deep neural network for hypersonic spatiotemporal turbulence prediction," *Phys. Fluids*, vol. 36, no. 5, May 2024, doi: 10.1063/5.0210966.
- [47] M. Zhang, Z. Zhang, X. Wang, Z. Liao, and L. Wang, "The Use of Attention-Enhanced CNN-LSTM Models for Multi-Indicator and Time-Series Predictions of Surface Water Quality," *Water Resour. Manag.*, vol. 38, no. 15, pp. 6103–6119, Dec. 2024, doi: 10.1007/s11269-024-03946-1.
- [48] F. A. Gers, J. Schmidhuber, and F. Cummins, "Learning to Forget: Continual Prediction with LSTM," *Neural Comput.*, vol. 12, no. 10, pp. 2451–2471, Oct. 2000, doi: 10.1162/089976600300015015.
- [49] A. Graves, "Generating Sequences With Recurrent Neural Networks," Jun. 2014, [Online]. Available: <http://arxiv.org/abs/1308.0850>.
- [50] F. A. Gers and J. Schmidhuber, "Recurrent nets that time and count," in *Proceedings of the IEEE-INNS-ENNS International Joint Conference on Neural Networks. IJCNN 2000. Neural Computing: New Challenges and Perspectives for the New Millennium*, 2000, pp. 189–194 vol.3, doi: 10.1109/IJCNN.2000.861302.
- [51] R. K. Srivastava, K. Greff, and J. Schmidhuber, "Highway Networks," Nov. 2015, [Online]. Available: <http://arxiv.org/abs/1505.00387>.
- [52] S. Merity, N. S. Keskar, and R. Socher, "Regularizing and Optimizing LSTM Language Models," Aug. 2017, [Online]. Available: <http://arxiv.org/abs/1708.02182>.
- [53] R. Pascanu, T. Mikolov, and Y. Bengio, "On the difficulty of training Recurrent Neural Networks," Feb. 2013, [Online]. Available: <http://arxiv.org/abs/1211.5063>.
- [54] M. Schuster and K. K. Paliwal, "Bidirectional recurrent neural networks," *IEEE Trans. Signal Process.*, vol. 45, no. 11, pp. 2673–2681, 1997, doi: 10.1109/78.650093.
- [55] W. Li, F. Qi, M. Tang, and Z. Yu, "Bidirectional LSTM with self-attention mechanism and multi-channel features for sentiment classification," *Neurocomputing*, vol. 387, pp. 63–77, Apr. 2020, doi: 10.1016/j.neucom.2020.01.006.
- [56] Y. Yu, X. Si, C. Hu, and J. Zhang, "A Review of Recurrent Neural Networks: LSTM Cells and Network Architectures," *Neural Comput.*, vol. 31, no. 7, pp. 1235–1270, Jul. 2019, doi: 10.1162/neco_a_01199.
- [57] R. L. Abduljabbar, H. Dia, and P.-W. Tsai, "Unidirectional and Bidirectional LSTM Models for Short-Term Traffic Prediction," *J. Adv. Transp.*, vol. 2021, pp. 1–16, Mar. 2021, doi: 10.1155/2021/5589075.
- [58] M. L., Andrew, D. Raymond E., P. Peter T., H. Dan, Y. N. Andrew, and P. Christopher, "Learning Word Vectors for Sentiment Analysis Andrew," in *Proceedings of the 49th Annual Meeting of the Association for Computational Linguistics: Human Language Technologies*, 2011, vol. 47, no. 423, pp. 142–150.
- [59] Z. Shaukat, A. A. Zulfiqar, C. Xiao, M. Azeem, and T. Mahmood, "Sentiment analysis on IMDB using lexicon and neural networks," *SN Appl. Sci.*, vol. 2, no. 2, Feb. 2020, doi: 10.1007/s42452-019-1926-x.
- [60] S. M. Y. Iqbal Tomal, "Sentiment Analysis of IMDb Movie Reviews," *Int. J. Innov. Sci. Res. Technol.*, vol. 16, no. 1, pp. 2338–2343, 2024, doi: 10.38124/ijisrt/ijisrt24may1625.
- [61] D. M. Ulya, J. Juhari, R. E. Yuliana, and M. Jamhuri, "Reliable and Efficient Sentiment Analysis on IMDb with Logistic Regression," *CAUCHY J. Mat. Murni dan Apl.*, vol. 10, no. 2, pp. 821–834, Aug. 2025, doi: 10.18860/cauchy.v10i2.33809.
- [62] S. K. Singh and N. Singla, "Sentiment Analysis on IMDB Review Dataset," *J. Comput. Mech. Manag.*, vol. 2, no. 6, pp. 18–29, Dec. 2023, doi: 10.57159/gadl.jcmm.2.6.230108.
- [63] J. Lu, H. Fan, and Y. Zhang, "Sentiment Analysis of IMDB Movie Reviews Based on LSTM," *J. Adv. Eng. Technol.*, vol. 2, no. 2, Jun. 2025, doi: 10.62177/jaet.v2i2.429.
- [64] M. T. Islam, F. Parvin, S. A. Sazan, and T. Bin Amir, "Comparative Analysis of Sentiment Classification on IMDB 50k Movie Reviews: A Study Using CNN, LSTM, CNN-LSTM, and BERT Models," in *PEEIACON 2024 - International Conference on Power, Electrical, Electronics and Industrial Applications*, Sep. 2024, pp. 512–517, doi: 10.1109/PEEIACON63629.2024.10800035.
- [65] T. Wolf *et al.*, "Transformers: State-of-the-Art Natural Language Processing," in *Proceedings of the 2020 Conference on Empirical Methods in Natural Language Processing: System Demonstrations*, 2020, pp. 38–45, doi: 10.18653/v1/2020.emnlp-demos.6.
- [66] R. Sennrich, B. Haddow, and A. Birch, "Neural Machine Translation of Rare Words with Subword Units," Jun.

- 2016, [Online]. Available: <http://arxiv.org/abs/1508.07909>.
- [67] T. Akiba, S. Sano, T. Yanase, T. Ohta, and M. Koyama, "Optuna," in *Proceedings of the 25th ACM SIGKDD International Conference on Knowledge Discovery & Data Mining*, Jul. 2019, pp. 2623–2631, doi: 10.1145/3292500.3330701.
- [68] D. M. W. Powers, "Evaluation: from precision, recall and F-measure to ROC, informedness, markedness and correlation," Oct. 2020, [Online]. Available: <http://arxiv.org/abs/2010.16061>.
- [69] T. Fawcett, "An introduction to ROC analysis," *Pattern Recognit. Lett.*, vol. 27, no. 8, pp. 861–874, Jun. 2006, doi: 10.1016/j.patrec.2005.10.010.

Appendix

Appendix A.1: Language Modeling Evaluation on WikiText-103

The performance of long-range modeling was evaluated through standard language modeling metrics which were applied to the WikiText-103 validation split. The average cross-entropy loss as defined in Eq. A01, evaluates the model’s predictive uncertainty at the token level through, which functions as the main evaluation metric. The predictive difficulty measure known as perplexity emerges directly from this quantity (see Eq. A02). The information-theoretical token coding cost emerges is defined in Eq. A03 which shows the average number of bits required to encode each token. The token-level accuracy measurement (Eq. A04) determines the proportion of correct next-token predictions. The model achieves its sequence prediction and long-term context maintenance capabilities through the combination of these performance metrics.

$$L_{CE} = \frac{1}{T} \sum_{t=1}^T \log p\theta(y_t|x) \quad (\text{A01})$$

$$PPL = \exp(L_{CE}) \quad (\text{A02})$$

$$BPC = \frac{L_{CE}}{\ln 2} \quad (\text{A03})$$

$$Accuracy = \frac{1}{T} \sum_{t=1}^T 1(\hat{y}_t = y_t) \quad (\text{A04})$$

The performance results for WikiText-103 language modeling are shown in Table A1-1. The GRU and vanilla LSTM recurrent models showed their standard behavior because the LSTM outperforms GRU in both perplexity (91.45) and token accuracy despite having equal parameter numbers. The BiLSTM model achieves the best results in both perplexity (≈ 1.01) and token accuracy (≈ 0.99) but needs more than 80M parameters and results in a model size exceeding 300 MB. The model becomes unsuitable for environments with limited resources and real-time applications because its performance gain from bidirectional recurrence requires significant computational power. The QL-LSTM variants demonstrate how various architectural elements affect both model performance results and operational efficiency throughout the model structure.

- PSUG-only proved that parameter-shared gating enables the model to decrease its parameter count to 26M while achieving acceptable perplexity results, which demonstrates unified gating effectiveness for lightweight recurrent modeling.
- The HGR-ASC-only achieves the highest token-level performance among QL-LSTM variants through its block-level skip recurrence mechanism which helps stabilize long-range information transmission.
- The QL-LSTM model with PSUG and HGR-ASC achieves a middle ground in performance by reaching 131.88 perplexity and using 34M parameters while keeping the model size at 132 MB. The model produces superior results than BiLSTM while preserving causal boundaries which enables it for various upcoming applications.

The results demonstrate that QL-LSTM enables designers to select between three optimization approaches through PSUG for parameter minimization and HGR-ASC for better context management and easier recurrent structure design which generates more reliable outcomes than standard models. The results prove QL-LSTM functions as the best solution for sequence modeling tasks which require fast processing, causal analysis and deep contextual understanding.

Table A1-1: Performance evaluation between the baseline RNN models and QL-LSTM trained and evaluated on WikiText-103 data with a maximum sequence length of 256.

Model	Loss	Perplexity	Bits/Token	Token Accuracy	Num Params	Size (MB)	Epoch
GRU	6.54	689.55	9.43	0.19	27,357,777	104.36	5
BiLSTM	0.01	1.01	0.02	0.99	81,447,505	310.70	5
Vanilla LSTM	4.52	91.45	6.51	0.30	27,883,089	106.37	5
QL-LSTM							
• HGR-ASC-only	4.62	101.64	6.67	0.29	36,271,185	138.36	5
• PSUG-only	4.0	132.66	7.05	0.27	26,308,177	100.36	5
• Full: PSUG+HGR	4.88	131.88	7.04	0.27	34,698,321	132.36	5

Appendix A2: Optuna Hyperparameter Search Results for QL-LSTM (Performance Metrics in Percentage)

Trial	Emb	Hidden	Leap	Pool	MaxLen	Batch	LR	WDecay	Params (M)	Size (MB)	Test Acc (%)	Test F1 (%)	ROC AUC (%)	Best Val Acc (%)	Avg Epoch (s)	Peak GPU (MB)
0	512	256	64	max	384	64	1.15e-03	5.21e-05	30.12	114.9	86.04	86.01	94.10	87.44	185.7	762.4
1	384	512	64	mean	256	16	2.02e-05	3.62e-05	36.54	139.4	75.47	75.41	84.10	76.16	295.6	716.2
2	256	512	32	mean	384	32	9.35e-04	1.25e-04	21.65	82.6	85.88	85.86	93.79	88.12	226.1	603.1
3	512	512	64	mean	256	64	2.37e-04	3.01e-06	43.04	164.2	82.98	82.94	91.30	84.32	115.5	1019.4
4	256	512	32	mean_max	384	64	1.19e-04	6.50e-04	21.65	82.6	80.18	80.14	88.58	81.16	167.0	854.9
6	512	256	32	mean_max	512	32	1.36e-03	2.48e-04	28.03	106.9	85.83	85.83	93.23	87.90	379.6	637.3
7	512	384	64	mean	384	32	9.47e-04	3.52e-06	35.52	135.5	85.26	85.25	92.96	88.16	263.2	761.0
9	512	256	16	mean	384	16	8.71e-04	1.36e-04	26.98	102.9	85.73	85.72	93.47	88.08	455.1	531.9
13	256	512	32	mean	384	32	3.19e-03	8.70e-03	21.65	82.6	86.36	86.35	93.70	88.52	228.0	603.1
14	256	384	16	mean	512	32	4.96e-03	8.63e-03	15.47	59.0	87.70	87.70	94.67	88.94	316.1	515.7
15	256	512	16	mean_max	512	32	3.04e-03	8.61e-03	17.46	66.6	86.69	86.69	93.89	88.22	349.4	626.7
16	256	384	16	mean	512	16	4.57e-03	9.03e-03	15.47	59.0	87.83	87.82	94.83	89.08	592.6	387.4

Appendix A3: The figure demonstrates how different architectural parameters (embedding size, hidden dimension, leap interval, pooling method, parameter count) and optimization parameters (learning rate, batch size) affect the performance metrics of QL-LSTM which include test accuracy, F1-score, ROC-AUC, training speed and GPU memory usage. The plots collectively demonstrate the parameter-efficiency, long-range modeling behavior, and stability of QL-LSTM across diverse configurations.

